

Catalytic Features of Phenolic Acid Decarboxylase

from *Candida guilliermondii*

(*Candida guilliermondii* 由来のフェノール酸脱炭酸酵素に関する研究)

Hui-Kai Huang

2012

Catalytic Features of Phenolic Acid Decarboxylase
from *Candida guilliermondii*

(*Candida guilliermondii* 由来のフェノール酸脱炭酸酵素に
関する研究)

Hui-Kai Huang

A dissertation submitter to the United Graduate School of
Agricultural Sciences, Kagoshima University, Japan, in partial
fulfillment of the requirement for the degree of

DOCTOR OF PHILOSOPHY

in Agricultural Science

2012

Contents

Chapter 1	General Introduction	1
Chapter 2	Purification and properties of phenolic acid decarboxylase from <i>Candida guilliermondii</i>	4
2-1	Introduction.....	4
2-2	Materials and methods	5
2-3	Results.....	9
Chapter 3	An endogenous factor enhances ferulic acid decarboxylation catalyzed by phenolic acid decarboxylase from <i>Candida guilliermondii</i>	23
3-1	Introduction.....	23
3-2	Materials and methods	24
3-3	Results.....	29
Chapter 4	Discussion	45
Summary	51
References	52
Acknowledgements	60

Abbreviations

FA, ferulic acid

PCA, *p*-coumaric acid

CA, caffeic acid

4-VG, 4-vinylguaiacol

4-VP, 4-vinylphenol

6H2N, 6-hydroxy-2-naphthoic acid

PAD, phenolic acid decarboxylase

CgPAD, PAD from *C. guilliermondii*

PMSF, phenylmethanesulfonyl fluoride

MES, 2-morpholinoethanesulfonic acid

SDS-PAGE, SDS-polyacrylamide gel electrophoresis

HPLC, high-performance liquid chromatography

SD, standard deviation

YNB, Yeast Nitrogen Base

DTNB, 5,5'-dithio-bis(2-nitrobenzoic acid)

Chapter 1 Introduction

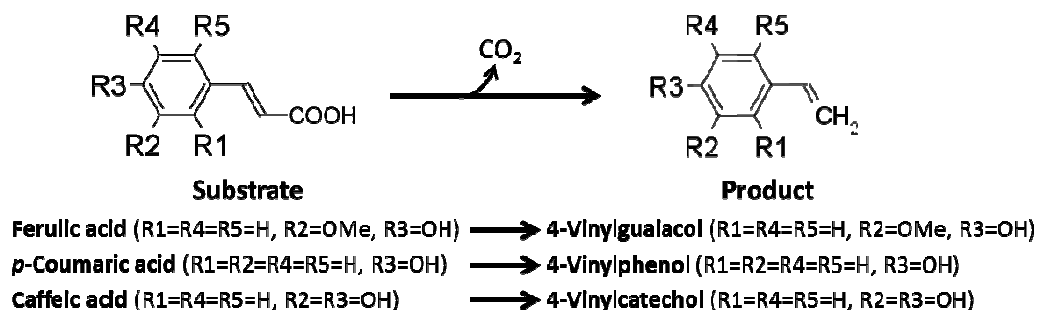
Phenolic acids are components of phenolic ring and an organic carboxylic acid function. They are widely distributed plant constituents. Phenolic acids can be subdivided into two major groups, hydroxybenzoic acids and hydroxycinnamic acids. Hydroxybenzoic acids include *p*-hydroxybenzoic, protocatechuic, vanillic, syringic, and gallic acids. They are commonly present in the bound form and are typically a component of a complex structure like lignins and hydrolyzable tannins. Hydroxycinnamic acids include *p*-coumaric, caffeic, ferulic, and sinapic acids. They are mainly found esterified with small molecules, e.g., quinic or tartaric acids, as well as cell-wall-bound structural components, such as cellulose, lignin, and proteins, through ester bonds (Liu 2004).

Ferulic acid (FA), a derivative of hydroxycinnamic acid, is found in cell walls, leaves and seeds of plants such as in rice, wheat, and oat, as well as in coffee, apple, artichoke, peanut, orange, and pineapple (Mathew and Abraham 2004). It occurs in them primarily in both its free form and as an ester linked to lignin and other polysaccharides. FA is a precursor to vanillin, one of the aromatic flavors used in the food, pharmaceutical, and cosmetic industries (Mathew and Abraham 2006; Priefert et al. 2001). In addition, due to both its antioxidant and anti-inflammatory activities, FA has versatile functional and biological activities, such as protecting foods from oxidative spoilage (Maoka et al. 2008) and whitening skin (Lin et al. 2005), and it has been shown to lower blood glucose level, blood pressure (Ardiansyah et al. 2008; Mathew and Abraham 2004), plasma total cholesterol and low-density-lipoprotein cholesterol concentrations (Jung et al. 2007; Sri Balasubashini et al. 2003), and inhibit tumor promotion (Huang et al. 1988).

Volatile phenols, including 4-vinylguaiacol (4-VG), 4-vinylphenol (4-VP), and ethylphenol, are frequently detected in beer, wine, and whiskey during brewing and fermentation. These phenolic compounds usually originate from the microbial decarboxylation of phenolic acids (hydroxycinnamic acids) present in the raw materials during fermentation (Coghe et al. 2004; Sáez et al. 2010; Smit et al. 2003; Van Beek and Priest 2000; Vanbeneden et al. 2008) and in fruit juice production (Donaghy et al. 1999; Fallico et al. 1996). They are valuable precursors in the biotransformation of flavors and fragrances (Mathew and Abraham 2006; Priefert et al. 2001) and are regarded as a good aroma and/or off-flavors in beers and wines (Coghe et al. 2004; Oelofse et al. 2008; Sáez et al. 2010; Smit et al. 2003; Thurston and Tubb 1981; Vanbeneden et al. 2008). The 4-VG formed is valuable precursor in the biotransformation of flavors and fragrances used in the food, pharmaceutical, and cosmetic industries (Mathew and Abraham 2006; Priefert et al. 2001).

The microbial phenolic acid decarboxylases (PADs), which decarboxylate FA and/or *p*-coumaric acid (PCA) with concomitant production of 4-VG and/or 4-VP, respectively, are believed to be responsible for the detoxification of phenolic acids (Cavin et al. 1997b, 1998; Clausen et al. 1994; Coghe et al. 2004; Degrassi et al. 1995; Huang et al. 1994; Smit et al. 2003). Namely, bacterial PADs, which decarboxylate FA, PCA, and/or caffeic acid (CA) with concomitant production of 4-VG, 4-VP, and/or 4-vinylcatechol, respectively (see below), are responsible for the detoxification of these 4-hydroxycinnamic acids (Huang et al. 1994; Degrassi et al. 1995; Cavin et al. 1997b, 1998). Zago et al. (1995) first succeeded in sequencing and expression of a bacterial PAD (FA decarboxylase from *Bacillus pumilus*) in *Escherichia coli*. The genetic mechanism of bacterial PAD expression has been well established by the discovery of PadR-mediated response to 4-hydroxycinnamic acids in *Pediococcus pentosaceus* (Barthelmebs et al. 2000b), *Bacillus subtilis* (Tran et al. 2008), and *Lactobacillus plantarum*

(Gury et al. 2009).



Reaction scheme for CgPAD with different substrates

Naturally-occurring phenolic acids are known to inhibit the growth of yeasts such as *Saccharomyces cerevisiae*, *Pichia anomala*, *Debaryomyces hansenii*, and *Candida guilliermondii* (*Meyerozyma guilliermondii* comb. nov.; Kurtzman and Suzuki 2010) (Baranowski et al. 1980, Pereira et al. 2011, Stead 1995). *S. cerevisiae* (Goodey and Tubb 1982; Clausen et al. 1994; Smit et al. 2003; Coghe et al. 2004), *Brettanomyces bruxellensis* (Godoy et al. 2008) are suggested to produce a PAD in response or relation to 4-hydroxycinnamic acids. *C. guilliermondii* has been frequently isolated from grapes and musts as a contaminant (Barata et al. 2008; Dias et al. 2003; Martorell et al. 2006). *Candida* spp. have been demonstrated to decarboxylate FA, generating 4-VG as an off-flavor in improperly stored fruit juices (Sutherland et al. 1995) and as a characteristic flavor of soy sauce and miso (Suezawa and Suzuki 2007).

However, little is known about the enzymatic properties of PADs from yeasts except for those of the two species of *Brettanomyces* (Edlin et al. 1998; Godoy et al. 2008). The aim of this work was to purify and characterize, and cloning and sequencing the gene for a PAD from *C. guilliermondii* ATCC 9058 (CgPAD), which may be involved in the metabolism of phenolic acids by yeast.

Chapter 2 Purification and properties of phenolic acid decarboxylase from *Candida guilliermondii*

2-1 Introduction

FA, a derivative of hydroxycinnamic acid, is found in cell walls, leaves and seeds of plants such as in rice, wheat, and oat, as well as in coffee, apple, artichoke, peanut, orange, and pineapple (Mathew and Abraham 2004). It occurs in them primarily in both its free form and as an ester linked to lignin and other polysaccharides. FA is a precursor to vanillin, one of the aromatic flavors used in the food, pharmaceutical, and cosmetic industries (Mathew and Abraham 2006; Priefert et al. 2001). In addition, due to both its antioxidant and anti-inflammatory activities, FA has versatile functional and biological activities, such as protecting foods from oxidative spoilage (Maoka et al. 2008) and whitening skin (Lin et al. 2005), and it has been shown to lower blood glucose level, blood pressure (Ardiansyah et al. 2008; Mathew and Abraham 2004), plasma total cholesterol and low-density-lipoprotein cholesterol concentrations (Jung et al. 2007; Sri Balasubashini et al. 2003), and inhibit tumor promotion (Huang et al. 1988).

Volatile phenols, including 4-VG, 4-VP, and ethylphenol, are frequently detected in beer, wine, and whiskey during brewing and fermentation. These phenolic compounds usually originate from the microbial decarboxylation of phenolic acids (hydroxycinnamic acids) present in the raw materials during fermentation (Coghe et al. 2004; Sáez et al. 2010; Smit et al. 2003; Van Beek and Priest 2000; Vanbeneden et al. 2008) and in fruit juice production (Donaghy et al. 1999; Fallico et al. 1996). They are valuable precursors in the biotransformation of flavors and fragrances (Mathew and Abraham 2006) and are regarded as a good aroma and/or off-flavors in beers and wines (Coghe et al. 2004; Oelofse et al. 2008; Sáez et al. 2010; Smit et al. 2003;

Thurston and Tubb 1981; Vanbeneden et al. 2008). The microbial PADs, which decarboxylate FA and/or PCA with concomitant production of 4-VG and/or 4-VP, respectively, are believed to be responsible for the detoxification of phenolic acids (Cavin et al. 1997b, 1998; Clausen et al. 1994; Coghe et al. 2004; Degrassi et al. 1995; Huang et al. 1994; Smit et al. 2003).

The aim of work in this chapter was to purify and characterize a CgPAD, which may be involved in the metabolism of phenolic acids by yeast.

2-2 Materials and methods

Materials

FA, CA, 4-VG, and 6-hydroxy-2-naphthotic acid (6H2N) were purchased from Wako Pure Chemical (Osaka, Japan). PCA was from MP Biomedicals (Solon, OH), and 4-VP was from Sigma-Aldrich (Steinheim, Germany). All other chemicals used were of analytical grade.

Organism and culture conditions

The enzyme source was *C. guilliermondii* ATCC 9058. The growth medium (w/v) was composed of 1.0% glucose, 0.5% peptone (Bacto Peptone; Becton, Dickinson and Company, Sparks, MD), 0.2% yeast extract (Becton, Dickinson and Company). 0.1% K₂HPO₄, 0.1% K₂HPO₄, 0.01% MgSO₄·7H₂O, and 1 mM 6H2N (pH 7.0). The yeast was grown at 25°C for 3 days, with shaking, in 200-ml aliquots of the medium placed in 2-l flasks. After collecting cells by centrifugation (3,000 × g for 5 min) at 4°C, the cell paste (17.7 g wet wt. from 600-ml culture) was used as the starting material for purification of the enzyme. 6H2N was used as the pseudo-inducer because our preliminary experiments showed that it enhanced the expression of the enzyme in the cells much more than FA and PCA did.

Purification of CgPAD

Enzyme purification was done at a temperature not exceeding 4°C.

Step 1 Preparation of cell-free extract

The harvested 6H2N-induced cells were washed twice with saline and then suspended in 20 mM sodium phosphate buffer (pH 7.0) containing 1 mM each of phenylmethanesulfonyl fluoride (PMSF), MgCl₂, EDTA, and dithiothreitol. The yeast cells were disrupted six times for 50 s each with glass beads (0.5 mm in diameter) at 2,500 rpm in a homogenizer (Multi-Beads Shocker; Yasui Kikai, Osaka, Japan). After cell debris was removed by centrifugation (12,000 × g, 15 min), the supernatant obtained was used as cell-free extract.

Step 2 Cation exchange chromatography

The cell-free extract was applied directly to a column of CM Toyopearl 650M (2.5 cm × 24 cm; Tosoh, Tokyo, Japan) previously equilibrated with 20 mM 2-morpholinoethanesulfonic acid (MES) buffer (pH 6.0). Proteins containing CgPAD were eluted with the buffer.

Step 3 Anion exchange chromatography

The active fractions that passed through the column were combined, and the solution was immediately applied to a column of DEAE Sepharose Fast Flow (2.5 cm × 25.5 cm; GE Healthcare) equilibrated with the same buffer. The column was initially washed with 700 mL of 50 mM NaCl in MES buffer (pH 6.0), and proteins were eluted with a 600-ml linear gradient of 50 mM to 400 mM NaCl in the buffer (Fig. 2-1).

Step 4 Gel-filtration chromatography

The active fractions were concentrated and exchanged with 50 mM phosphate buffer (pH 7.0) by ultrafiltration (Amicon Ultra-15; Millipore, Billerica, MA) to a small volume. The concentrate was then put on a column of Bio-Gel P-100 (2.5 cm × 45 cm; Bio-Rad, Hercules, CA) equilibrated with 50 mM sodium phosphate buffer (pH 7.0). The gel-filtration

chromatography was done by elution with the equilibration buffer, and the active fractions eluted were combined and concentrated by ultrafiltration (Fig. 2-2). The resultant retentate was used exclusively for further experiments as the final preparation of purified enzyme. The purified enzyme was stored at -20°C when necessary.

Estimation of molecular mass

SDS-polyacrylamide gel electrophoresis (SDS-PAGE) was done using a 15% (w/v) acrylamide gel for determination of the subunit molecular mass. Proteins in the gel were stained with Coomassie Brilliant Blue R250. The subunit molecular mass was determined using a PageRuler Unstained Protein Ladder kit (Thermo Fisher Scientific, Rockville, MD). The molecular mass of the native form was estimated by gel-filtration chromatography using a column of Superdex75 10/300 GL (GE Healthcare & Bio-Sciences, Uppsala, Sweden) at a flow rate of 0.4 ml/min (L-7100 pump; Hitachi, Tokyo, Japan) with 50 mM phosphate buffer plus 0.15 M NaCl (pH 7.0). The column was calibrated with standard molecular mass markers (Sigma-Aldrich), bovine serum albumin (66 kDa), chicken egg albumin (44 kDa), carbonic anhydrase (29 kDa), and cytochrome *c* (12.4 kDa), using a UV detector operated at 220 nm (U-VIS L-7420; Hitachi).

Assay of CgPAD activity

The initial velocity of decarboxylation activity was measured at 25°C with phenolic acids as substrates unless otherwise stated. The reaction mixture contained suitably-diluted enzyme solution and a 5 mM substrate (neutralized with 1.0 N NaOH) in 100 mM sodium phosphate buffer (pH 6.0) in a final volume of 1.0 ml. The products formed were quantified by

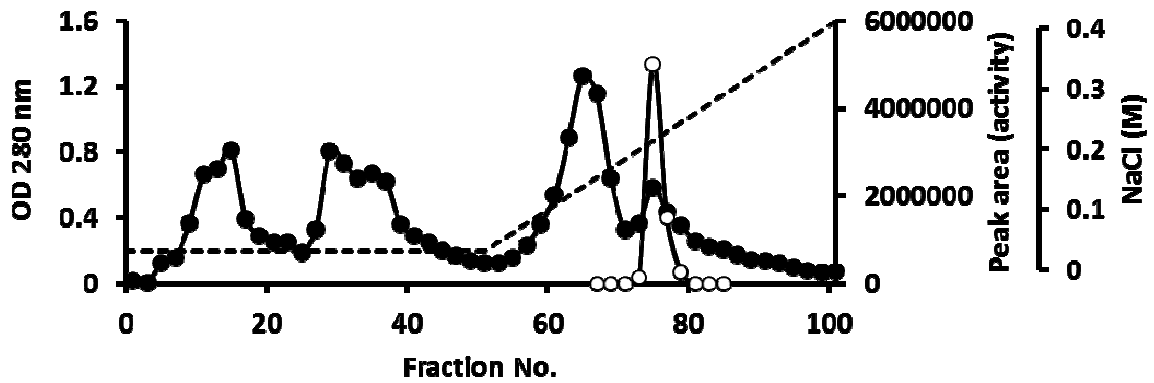


Fig. 2-1 Column chromatography on DEAE Toyopearl Fast Flow. The detailed procedures are described in the text. ●, A_{280} ; ○, FA activity; dotted line, NaCl concentration. Twelve-ml eluate was collected in each fraction tube.

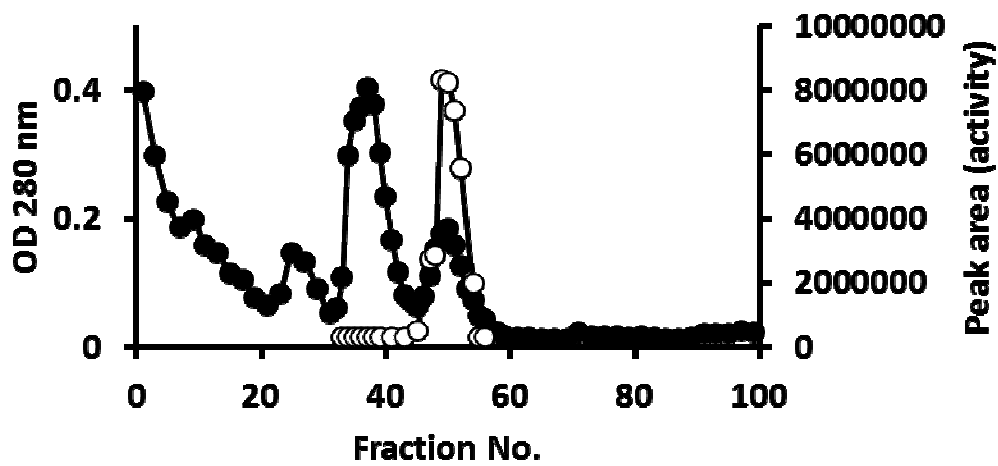


Fig. 2-2 Gel chromatography on Bio-Gel P-100. The detailed procedures are described in the text. ●, A_{280} ; ○, FA activity. Two-ml eluate was collected in each fraction tube.

high-performance liquid chromatography (HPLC) on an HPLC system from Waters (Milford, MA) equipped with a 2487 Dual λ Absorbance Detector and a 2695 Separation Module.

HPLC was done at 40°C on a packed column for reversed phase chromatography (Cosmosil 5C18-MS-II, 4.6 mm \times 150 mm; Nacalai Tesque, Tokyo, Japan) with acetonitrile/0.05% phosphoric acid (7:3, v/v) as the mobile phase at a flow rate of 0.6 ml/min. Ten μ l of the sample were injected automatically, and the UV detector was operated at 260 nm. One unit of enzyme activity was defined as the amount of enzyme that released 1 μ mol of 4-VG or 4-VP per min. Protein concentrations were measured with a BCA protein assay kit (Thermo Fisher Scientific) with bovine serum albumin as the standard.

Induction experiments

Yeast Nitrogen Base (YNB; Invitrogen, Carlsbad, CA) broth was used to induce the CgPAD. The carbon sources used were glucose, galactose, and sodium acetate at 0.5% (w/v) each, and inducer candidates were FA, PCA, and 6H2N each at 1.0 mM. Cultures were incubated at 25°C for 2 days, and the growth (A_{650}), pH of the spent media, and specific activities toward FA and PCA in the cell-free extracts were measured.

2-3 Results

Purification and physicochemical properties of CgPAD

A highly purified enzyme was obtained within 3 days by a simple purification procedure, as summarized in Table 2-1, with a high yield (19%). Approximately 87-fold purification to a specific activity of 531 U/mg was obtained when measured with FA as the substrate at 25°C in 0.1 M phosphate buffer at pH 6.0.

The protein was homogeneous, and its molecular mass determined to be approximately 20 kDa, as judged by SDS-PAGE (Fig. 2-3a). Gel chromatography of the purified enzyme gave a molecular mass of approximately 36 kDa (Fig. 2-3b), suggesting that the enzyme is a dimeric form composed of two identical subunits.

The absorption spectrum in the UV region exhibited a simple protein peak around at 280 nm, and the extinction coefficient at A_{280} (10 g/l; light path, 1 cm) was 20.5 in 50 mM phosphate buffer (pH 7.0) when the protein was quantified using bovine serum albumin as the reference standard.

Effects of metal ions and chemical reagents on activity

The enzyme reaction was carried out in the presence of various cations (5 mM each) at 25°C for 5 min with FA as the substrate. Fe^{2+} , Ni^{2+} , Cu^{2+} , and Hg^{2+} ions completely inhibited the reaction. Zn^{2+} ions caused 29% inhibition. Ca^{2+} , Mn^{2+} , Co^{2+} , Fe^{3+} , and Al^{3+} ions had either no effect or a slightly inhibitory effect. The decarboxylation activities toward FA and PCA gradually increased with the increase in the concentration of Mg^{2+} ions. The activation maxima of 180% and 153%, respectively, of the control activity were reached at around 10 mM without the cation. The activation by the cation of CA decarboxylation fluctuated considerably, possibly due to the low activity.

The effects of chemical reagents were examined by the method of Igarashi et al. (1998). The activity was inhibited almost completely by 4-chloromercuribenzoate, *N*-bromosuccinimide, and diethyl pyrocarbonate, but not by *N*-ethylmaleimide and iodoacetate (0.5 mM) under the indicated conditions, as shown in Table 2-2. PMSF and EDTA were without effect on the activity.

Table 2-1 A summary of typical purification of CgPAD

Purification step	Total vol. (mL)	Total protein (mg)	Total act. (U)	Specific act. (U/mg)	Yield (%)	Fold
Cell-free extract	37.5	251	1530	6.09	100	1.0
Toyopearl CM	103	128	1170	9.12	76.5	1.5
DEAE Sepharose FF	37.0	9.81	323	32.9	21.1	5.4
Bio-Gel P-100	1.67	0.55	292	531	19.1	87.2

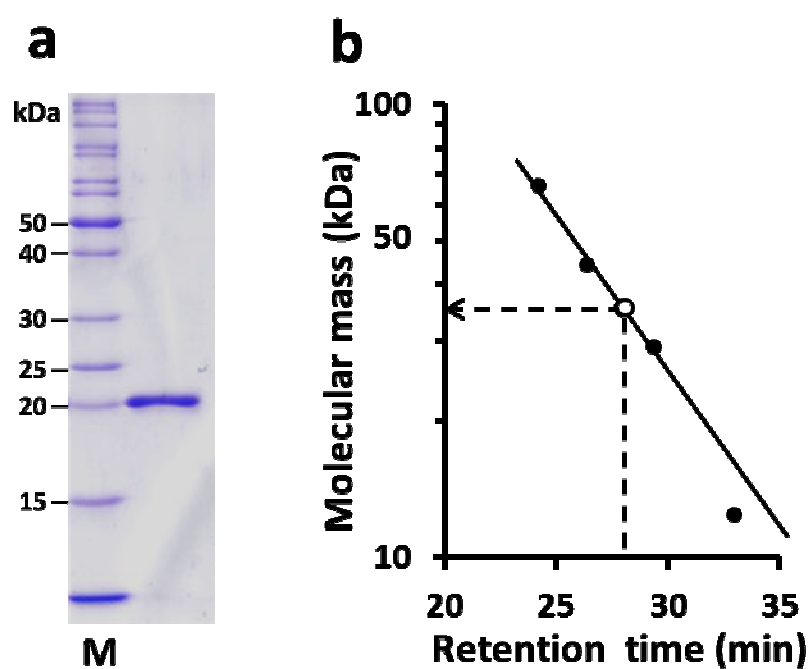


Fig. 2-3 Estimation of the molecular mass of the purified enzyme by SDS-PAGE (a) and gel-filtration chromatography (b). In a, *M* denotes molecular mass markers (in kDa), and the amount of the purified enzyme analyzed was 1.0 μ g.

Table 2-2 Effects of chemical reagents on the activity

Additive	Concentration (mM)	Relative activity ^a (%)
No additive		100 ± 11
<i>N</i> -Ethylmaleimide	1.0	96 ± 1.8
Diethyl pyrocarbonate	1.0	0
<i>N</i> -Bromosuccinimide ^b	0.1	4 ± 0.31
PMSF	1.0	94 ± 5.5
4-Chloromercuribenzoate ^c	0.5	7 ± 0.11
Iodoacetate ^c	0.5	84 ± 4.9
EDTA	1.0	99 ± 2.1

^a The activity was measured after the enzyme had been treated with each chemical reagent for 20 min at the indicated pH and temperature in the suitable buffer. The treatment conditions were at 25°C and at pH 6.0 in 10 mM phosphate buffer, and a 0.1-ml aliquot was used for the determination of the residual activity under the standard assay conditions. The values are the means of three experiments with standard deviation (SD) and shown as the percentages of the activity without additives, which is taken as 100%.

^b Treated for 20 min at 4°C and at pH 5.0 in 10 mM acetate buffer.

^c Treated for 20 min at 25°C and at pH 5.0 in 10 mM acetate buffer.

Substrate specificity and kinetic parameters

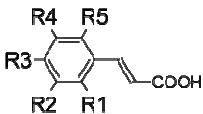
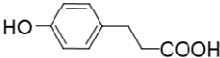
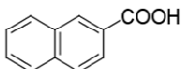
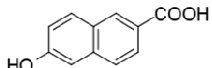
The purified CgPAD was examined for its ability to decarboxylate various phenolic acids and their derivatives (5 mM each) under the assay standard conditions. It decarboxylated PCA, FA, and CA at relative ratios of approximately 100:89:8, as shown in Table 2-3. No reaction was observed with cinnamic acid, 2- and 3-hydroxy-cinnamic acids, *o*- and *m*-cinnamic acids, 3-(4-hydroxyphenyl)-propionic acid, 2-naphthoic acid, and 6H2N. Among the active substrates, CgPAD tended to favor PCA over FA for catalysis, as judged by their K_m , k_{cat} , and catalytic efficiency (k_{cat}/K_m) values, as shown in Table 2-4. The k_{cat} for PCA with 5 mM Mg^{2+} ions was approximately 1.4-fold greater than that without the cation. The K_m values were not affected by the presence of the cation. These results suggested that this cation enhanced the CgPAD activity.

Effects of pH and temperature on activity and stability

The pH ranges at which the purified enzyme was active and stable were determined using FA as the substrate. As shown in Fig. 2-4a, the maximal activity was observed at pH 6.1 when measured in various buffers at 50 mM. When Britton-Robinson buffers at different pH values were used, the optimal pH was 5.9. In the pH range between 5.5 and 7.5, the specific activity was 2- to 4-fold greater in various buffers than that in Britton-Robinson buffers. In the buffers, no detectable activity was observed at lower than pH 4.3 and higher than pH 8.8. To determine the pH stability, the enzyme was preincubated at 4°C for 3 h in 10 mM Britton-Robinson buffer and assayed at 25°C in 0.1 M phosphate buffer at pH 6.0. The enzyme was stable over a range between pH 6.5 and 8.5, and the activity was completely abolished at pHs lower than 3.5 and higher than 11.5 (Fig. 2-5).

The decarboxylation activity was measured at various temperatures at pH 6.0 in 50 mM phosphate buffer in the absence or presence of 10 mM Mg^{2+} ions, as shown in Fig. 2-4b. The

Table 2-3 Substrate specificity of CgPAD

Substrate		Specific activity ^a (U/mg)	Relative activity (%)
Cinnamic acid (R1=R2=R3=R4=R5=H)		0	0
o-Coumaric acid (R2=R3=R4=R5=H, R1=OH)		0	0
m-Coumaric acid (R1=R3=R4=R5=H, R2=OH)		0	0
p-Coumaric acid (R1=R2=R4=R5=H, R3=OH)		600 ± 3.74	100
2-Hydroxy-cinnamic acid (R1=R2=R3=R4=H, R5=OH)		0	0
3-Hydroxy-cinnamic acid (R1=R2=R3=R5=H, R4=OH)		0	0
3-(4-Hydroxyphenyl)-propionic acid		0	0
Caffeic acid (R1=R4=R5=H, R2=R3=OH)		45.6 ± 2.47	7.6
Ferulic acid (R1=R4=R5=H, R2=OMe, R3=OH)		531 ± 31.9	88.5
2-Naphthoic acid		0	0
6-Hydroxy-2-naphthoic acid		0	0

^a Data represent the means of three experiments with SD.

Table 2-4 Kinetic parameters of CgPAD

Substrate	Kinetic parameter ^a		
	K_m (mM)	k_{cat} (s ⁻¹)	k_{cat}/K_m ^b (s ⁻¹ mM ⁻¹)
FA	5.32 ± 0.288	114 ± 2.67	21.4 ± 1.44
PCA	2.66 ± 3.91	113 ± 11.1	42.5 ± 3.06
PCA + 5 mM Mg ²⁺	2.64 ± 0.581	158 ± 22.0	59.8 ± 5.61

^a The values are the means of three experiments with SD and shown as the percentages of the activity without additives, which is taken as 100%.

^b The values were calculated assuming the native molecular mass as 36 kDa.

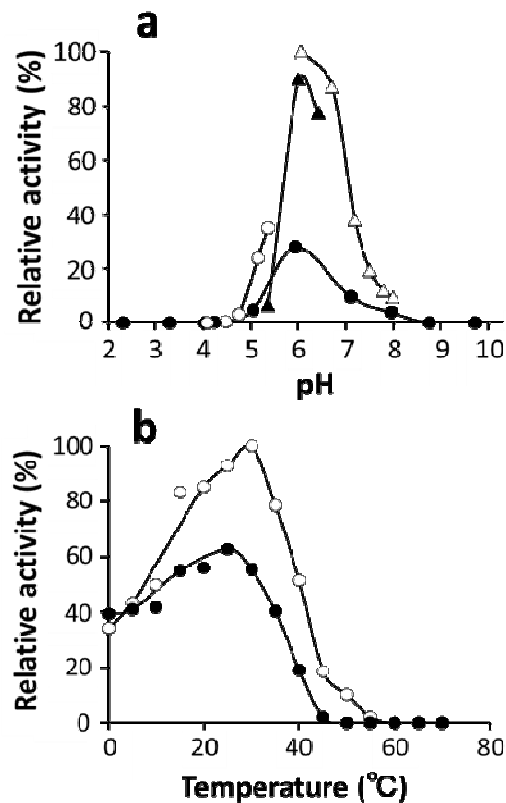


Fig. 2-4 Effects of pH and temperature on the activity of purified CgPAD. **a** The pH-activity curve was measured twice at 25°C with FA as substrate in various buffers at 50 mM (*open circle*, sodium acetate; *filled triangle*, MES; *open triangle*, sodium phosphate) and 50 mM Britton-Robinson universal buffers at different pH values (*filled circle*). The actual pH in each reaction mixture was previously measured at 25°C. The average values are expressed as percentages, taking the maximal activity as 100%. **b** The temperature-activity curves were measured at 25°C and at pH 6.0 in 50 mM phosphate buffer in the absence (*filled circle*) and presence of MgCl₂ (5 mM; *open circle*). The activities were measured twice at different temperatures under the standard conditions of enzyme assay using 0.1 M phosphate buffer (pH 6.0) with FA as substrate. The average values are expressed as percentages, taking the maximal activity as 100%.

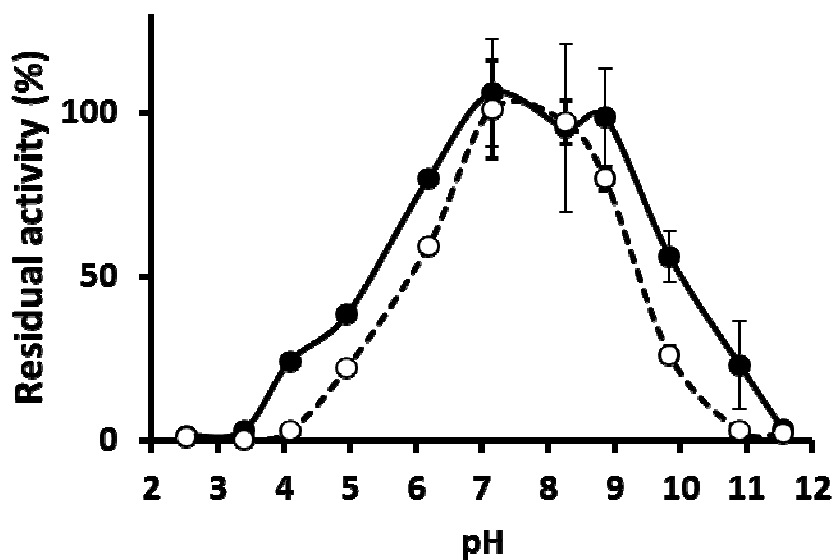


Fig. 2-5 pH stability at different pHs. The enzyme was treated at 4°C with 10 mM Britton-Robinson universal buffers at different pH values for 3 h (*filled circle*) and 16 h (*open circle*). The remaining activities were measured at 25°C with FA as substrate in sodium phosphate buffers at 50 mM. The values obtained from three separate experiments are shown and expressed as percentages, taking the maximal residual activity as 100%. The bars indicate the standard deviation at each point.

optimal temperature for activity with FA as the substrate was approximately 25°C, while that in the presence of Mg²⁺ ions was 25–30°C. The activity was stimulated by the divalent cation at the temperature range examined. Notably, even at 0°C, more than 50% of the activity at the optimal temperature was observed. The thermal stability of the enzyme was assessed at pH 6.0 in 50 mM phosphate buffer after heating for 20 min at various temperatures. The enzyme was stable up to 30°C (or more), and complete loss of activity was observed at 50°C, as shown in Table 2-5. At the temperatures examined, the ratios of remaining activity with and without 10 mM Mg²⁺ ions were essentially the same, indicating again that the cation causes activation of activity, but not protection from thermal inactivation.

Inducibility of CgPAD

In order to study the inducibility of CgPAD, we initially examined the effects of 0.5% (w/v) carbon sources on the expression of the enzyme in the YNB broth plus 1 mM 6H2N instead of the complex medium used for enzyme purification.

Under shaking conditions, the induction on glucose with 6H2N was approximately double those on galactose or sodium acetate after incubation at 25°C for two days. Then, we examined the effects of 1 mM each of 6H2N, FA, and PCA on the inducibility of CgPAD in YNB broth plus 0.5% glucose. As shown in Table 2-6, the addition of PCA or FA to the media induced FA and PCA activities at equal ratios. Unexpectedly, 6H2N was found to induce both activities at approximately 16-fold and 6-fold greater levels than FA and PCA, respectively. In addition, 6H2N-induced cells grown on glucose, galactose, and sodium acetate contained the decarboxylation activities toward PCA and FA at relative ratios of 1:3, 1:2, and 1:4, respectively. Notably, when glucose was used as a carbon source, the aerobic growth with PCA or FA was double that without the additive, while that with 6H2N did not.

Table 2-5 Thermal stability at different temperatures

Temperature (°C)	Relative activity (%) ^a		
	- Mg ²⁺	+ Mg ²⁺	+ Mg ²⁺ /- Mg ²⁺
Control	100 ± 11.4	135 ± 2.13	135 ± 2.13
25	107 ± 5.69	131 ± 1.18	122 ± 1.10
30	102 ± 1.56	140 ± 2.70	137 ± 2.60
40	67 ± 1.15	87 ± 8.92	130 ± 13.3
50	8 ± 0.26	7 ± 1.56	88 ± 19.6

^a The enzyme was pre-treated at the indicated temperatures for 20 min in the absence or presence of Mg²⁺ ions (5 mM) in 0.1 M phosphate buffer (pH 6.0). The residual activities were determined under the standard conditions of enzyme assay. The values are the means of three experiments with SD, taking the control (not heated) as 100%.

Table 2-6 Inducibility of CgPAD under different growth conditions

Growth condition ^a	Growth (A ₆₅₀)	pH of medium	Specific activity (U/mg) ^b		Ratio of FA/PCA
			FA	PCA	
Glucose					
+ no additive	8.6	2.4	0.24	0.33	0.73
+ 1 mM FA	15	2.3	0.72	0.94	0.77
+ 1 mM PCA	17	2.1	0.97	1.31	0.74
+ 1 mM 6H2N	6.7	2.6	16.7	6.11	2.73
Galactose					
+ 1 mM 6H2N	5.4	2.6	9.83	4.58	2.15
Sodium acetate					
+ 1 mM 6H2N	2.7	5.1	8.54	2.18	3.89

^a Each culture was grown with shaking in YNB broth plus 0.5% (w/v) carbon source at 25°C for 2 days.

^b The activities toward both substrates were measured twice, and the average values are shown.

Bioconversions of FA and PCA under growing conditions

C. guilliermondii ATCC 9058 was grown aerobically in YNB broth plus 0.5% (w/v) glucose with FA and PCA (each at 1 mM) under the same conditions as described above. The phenolic acids were converted almost stoichiometrically to 4-VG and 4-VP, respectively, within 24 h, as shown in Fig. 2-6. Further conversion of the two products did not occur even after 2 days. When anaerobiosis was attained in a flask, which was filled with the media up to the narrow neck, the amount of growth at A_{650} on 0.5% (w/v) glucose was faint and reached 0.2 after a 2-day and 0.5 even after a 5 day-incubation.

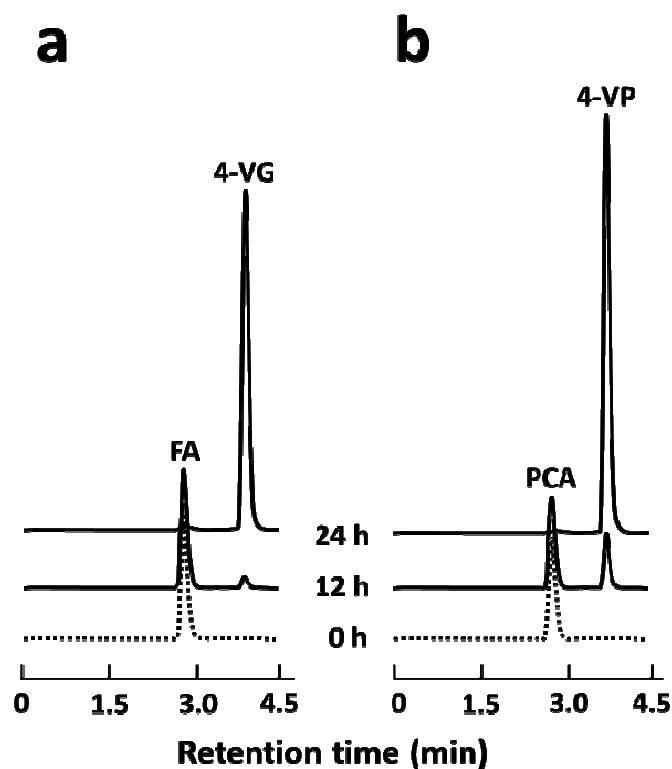


Fig. 2-6 Bioconversions of FA and PCA during the growth of *C. guilliermondii*. The yeast was grown with shaking at 25°C on 0.5% (w/v) glucose in YNB broth plus 1.0 mM each of FA and PCA. At intervals (12, 24, and 36 h), aliquots (10 μ l) of each broth were withdrawn and subjected to HPLC with the uninoculated broth as reference (0 h, *dotted line*). **a** Elution profiles of HPLC when FA was added. FA Retention times of FA and 4-VG were 2.83 and 3.90 min, respectively. **b** Those when PCA was added. Retention times of PCA and 4-VP were 2.79 and 3.75 min, respectively. The amounts of 4-VG and 4-VP accumulated after 24 h were calculated to be approximately 1 mM for both. The HPLC profiles after 36 h were similar to those after 24 h.

Chapter 3 An endogenous factor enhances ferulic acid decarboxylation catalyzed by phenolic acid decarboxylase from *Candida guilliermondii*

3-1 Introduction

The genetic mechanism of bacterial PAD expression has been well established by the discovery of PadR-mediated response to 4-hydroxycinnamic acids in *P. pentosaceus* (Barthelmebs et al. 2000b), *B. subtilis* (Tran et al. 2008), and *L. plantarum* (Gury et al. 2009). To understand the genetic feature of PADs, Zago et al. (1995) first succeeded in sequencing and expression of a bacterial PAD (FA decarboxylase from *B. pumilus*) in *Escherichia coli*.

CgPAD may be induced by both PCA and FA, because the ratios of decarboxylation activity toward FA to PCA in the cell-free extracts were comparable to that of the purified enzyme. However, 6-hydroxy-2-naphthoic acid (6H2N) induced CgPAD 20- and 6-fold greater than FA and PCA, respectively, and the ratios of decarboxylation activity toward FA to PCA in the cells grown on different carbon sources in the presence of the pseudo-inducer were found to be increased remarkably (see Chapter 2). There was a possibility that 6H2N induced another FA decarboxylase distinct from CgPAD under a defined condition, but such activity was not detectable during the course of purification.

In this chapter, to resolve this inconsistency, we sequenced the gene for CgPAD and created recombinant enzymes. Unexpectedly, we found that the presence of dithiothreitol, 2-mercaptoethanol, cysteine, and homocysteine considerably accelerated the rates of FA decarboxylation activity of the purified native and recombinant CgPAD, while they did not affect those of their PCA decarboxylation activity. We also demonstrated that an unidentified

amino thiol-like compound in the ultrafiltrate of the *C. guilliermondii* cell-free extract enhanced the FA decarboxylation activity specifically.

3-2 Materials and methods

Materials

FA, CA, 4VG, and 6H2N were purchased from Wako Pure Chemical (Osaka, Japan). PCA was from MP Biomedicals (Solon, OH), and 4VP was from Sigma-Aldrich (Steinheim, Germany). All other chemicals used were of analytical grade.

Microorganisms and propagation

The source of PAD and its gene was *C. guilliermondii* ATCC 9058. The enzyme was induced aerobically by 6H2N (1 mM) in YNB (Invitrogen, Carlsbad, CA) broth containing 0.5% glucose, as described in Chapter 2. Briefly, the yeast was grown at 25°C for 1 day, with shaking, in 200-ml portions of the medium placed in 2-l flasks. *Escherichia coli* DH5 α (Takara Bio, Otsu, Japan) and *E. coli* BL21 (DE3) (Takara Bio) were used for plasmid preparation and sequencing and for expression and purification of recombinant CgPAD, respectively.

The transformed *E. coli* cells were grown, with shaking, at 37°C in 50-ml portions of Luria-Bertani broth plus ampicillin (100 $\mu\text{g ml}^{-1}$) placed in 500-ml flasks to an A_{600} of 0.5. After adding isopropyl β -D-galactosyl pyranoside (0.1 mM) to the culture, incubations were further continued at 18°C for 24 h. After cells were collected by centrifugation (12,000 $\times g$ for 10 min) at 4°C, cell pastes obtained from 600-ml culture were used as the starting materials for enzyme purification.

Purification of native and recombinant forms of CgPAD

The wild-type and mutant recombinant enzymes highly expressed in *E. coli* cells, together with native enzyme, were each purified by essentially the same procedure as that described for the native enzyme (Chapter 2), including chromatographies on CM Toyopearl 650M, DEAE Toyopearl 650M, and Bio-Gel P-100 columns, as described in Chapter 2.

Assay of CgPAD activity

The enzyme assay method was essentially the same as that described in Chapter 2.

Sequencing of internal amino acid residues of CgPAD

Initially, peptides of native CgPAD were obtained by treatment with CNBr or *Staphylococcus aureus* V8 protease. The CNBr cleavage was done essentially by the method of Steers et al. (1965). One mg of CgPAD was dissolved in 0.2 ml of 70% formic acid and cleaved with an excess of CNBr at room temperature for 24 h. After the remaining CNBr was removed by a rotary evaporator, the reaction mixture was filtered on a column of TSK gel G2000SWXL (Tosoh, 0.78 × 30 cm) in 30% acetic acid. The digestion of CgPAD with V8 protease was performed at 37°C for 6 h in 50 mM ammonium bicarbonate buffer (pH 7.8) plus 4 M urea and 2 mM EDTA. The peptide fragments obtained were fractionated by reverse-phase chromatography on a C4 column (3.9 × 150 mm, Waters, Milford, MA). The amino acid sequences of peptides derived from CNBr or V8 protease digestion of native CgPAD were determined by automated sequential Edman degradation using a PPSQ-23A protein sequencing system (Shimadzu, Kyoto, Japan).

Cloning and sequencing of CgPAD gene

All primers used are presented in Table 3-1. By a reverse transcription polymerase chain reaction using appropriate degenerate primers, the internal cDNA fragments of CgPAD were sequenced. Total RNA was isolated from *C. guilliermondii* using an RNeasy kit (Qiagen, Valencia, CA). First-strand cDNA synthesis was performed with 5 µg of total RNA using a GeneRacer kit (Invitrogen, Carlsbad, CA) with oligo(dT) adaptor primer. The cDNA obtained was used as a template for PCR amplification with degenerate primers. The first PCR was performed with primers P1 (a forward primer designed from an internal LKNKHFOQTYDNGWKYEFHV) and P2 (a reverse primer designed from an internal AFSQGHWEHPEQAHGDKRED), and nested PCR was done with P1 and P3 (a reverse primer designed from an internal AFSQGHWEHPEQAHGDKRED) (the sequences used for primer design are underlined). The nested PCR product was then cloned into a pGEM-T vector (Promega, Madison, WI) and sequenced using the ABI Prism system (Model 310; Applied Biosystems, Foster City, CA).

To obtain the entire gene for CgPAD, both 5' and 3' rapid amplification of cDNA ends (RACE) were performed using a GeneRacer kit according to the manufacturer's instructions. The gene-specific primers P4 (first PCR) and P5 (nested PCR) were used for the 5'-RACE and the gene-specific primers P6 (first PCR) and P7 (nested PCR) for the 3'-RACE. Approximately 250 bp and 290 bp were amplified by 5'-RACE and 3'-RACE, respectively. Finally, a cDNA fragment containing the entire coding region of CgPAD cDNA was amplified using the forward primer P8 (designed from the 5'-RACE product) and reverse primer P9 (designed from the 3'-RACE product).

The nucleotide sequence of CgPAD was submitted to DDBJ under the accession number AB663499

Table 3-1 Primers for CgPAD cDNA cloning.

Primer	Sequence (5' → 3')
P1*	CARTAYACNTAYGAYAAAYGG
P2*	TRTCNCCRTGNGCYTG
P3*	YTCNGGRTGYTCCCARTG
P4	ATATCCAAAATCAACGACACAACGG
P5	CAGTTTCTTCTAACCAATTGACTTGCC
P6	GGCAAGTCAATTGGTTAGAAGAAACTG
P7	CCGTTGTGTCGTTGATTTTGGATAT
P8	ATGCCTACCAACCACTTATTGG
P9	GAACCTCATTGCTTCAATTC

* Degenerate primers designed by internal amino acid sequences of native CgPAD.

Site-directed mutagenesis

The entire CgPAD gene was amplified by PCR and cloned into the *NdeI/HindIII* site of pET-22b (+) (Novagen, Darmstadt, Germany), yielding the construct designated pPAD22b. Amino acid replacements were performed using a QuikChange II site-directed mutagenesis kit (Stratagene, La Jolla, CA). PCR was performed using PfuUltra HF DNA polymerase (Promega) with pPAD22b as the template. The primer sets used were 5'-CATGGGGGGGCCACTGGCTGGACGGCAC-3'/5'-GTGCCGTCCAGCCCAGTGGCCCCCATG-3' for the Met57→Leu (M57L) mutation, 5'-CATGGGGGGGCCAACGGCTGGACGGCAC-3'/5'-GTGCCGTCCAGCCCGTTGGCCCCCATG-3' for the M57T mutation, and 5'-CATGGGGGGGCCAGCGGCTGGACGGCAC-3'/5'-GTGCCGTCCAGCCCGCTGGCCCCCATG-3' for the M57A mutation (the underlined sequences indicate mutated codons). To express mutant proteins, the resulting plasmids harboring the respective mutated genes were each introduced into competent *E. coli* BL21 (DE3) cells.

Construction of model structure of CgPAD

The secondary structure of CgPAD was predicted by the method of Kabsch and Sander (1983). The deduced amino acid sequence of the enzyme was aligned with that of the crystal structure of a PAD (PCA decarboxylase) from *L. plantarum* (LpPAD; PDB code 2GC9) (Rodríguez et al. 2010). A model of the CgPAD structure built with method of homology modeling was constructed based on the structure of LpPAD (Sali et al. 1993). All data sets were processed on a Windows XP personal computer using the Discovery Studio software package (Accelrys, San Diego, CA). Distance between intramolecular sulfur atom of methionine and side-chain carbonyl oxygen atoms of glutamic acid or amide nitrogen atom of arginine was

calculated from the coordinate values. The figure was prepared using a DS Visualizer (Accelrys).

3-3 Results

Purification of native and recombinant forms of CgPAD

Highly purified recombinant wild-type and mutant enzymes were obtained within 2 d by the simple purification procedure (Fig. 3-1). All the recombinant enzymes were purified to homogeneity as judged by SDS-acrylamide gel electrophoresis approximately 2- to 5-folds with yields of 40–70%.

Nucleotide and deduced amino acid sequences of CgPAD

To resolve unusual inconsistency of the above-mentioned substrate specificity (see Table 2-6), we first sequenced the gene for CgPAD and created recombinant enzymes. We initially cloned and sequenced the CgPAD gene. The entire CgPAD gene was 504 nucleotides in length, and an open reading frame encoded 168 amino acid residues (Fig. 3-2). The calculated molecular mass was 19,828 Da (http://web.expasy.org/compute_pi/), a value very close to the 20 kDa determined for the native enzyme by SDS-PAGE.

The deduced amino acid sequence of CgPAD was aligned with those of functional PADs reported to date from different bacteria (Thompson et al. 1997; <http://www.genome.jp/tools-bin/clustalw>). As shown in Fig. 3-3, CgPAD exhibited very low similarity of sequence to functional PADs reported to date from *L. plantarum* WCFS1 (Rodríguez et al. 2010) and *L. plantarum* LPCHL2 (Cavin et al. 1997a) with 39%, *Enterobacter* sp. Px6-4 (Gu et al. 2011a, 2011b) with 34%, *K. oxytoca* (Uchiyama et al. 2008) with 27%, *B.*

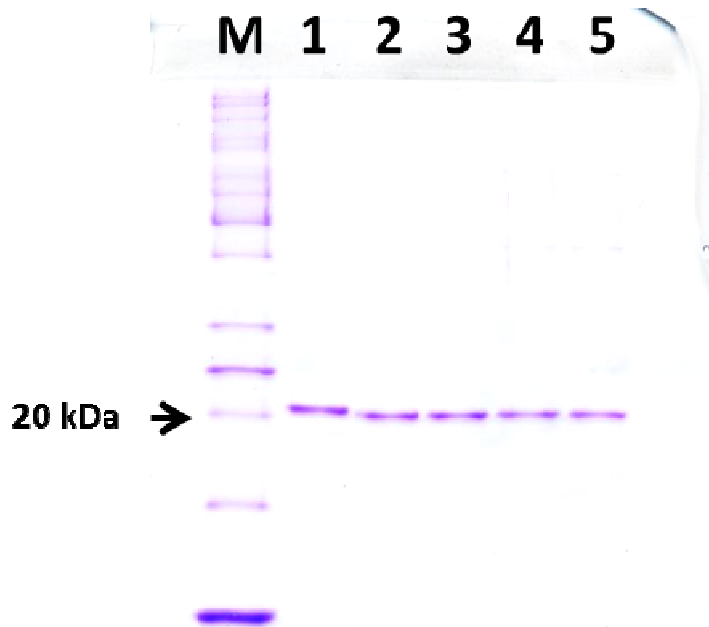


Fig. 3-1 SDS-PAGE of purified enzymes. The electrophoresis was done using a 15% (w/v) acrylamide gel for determination of the molecular masses, using a PageRuler Unstained Protein Ladder kit (Thermo Fisher Scientific, Rockville, MD) as standard markers. Proteins in the gel were stained with Coomassie Brilliant Blue R250. M, Molecular size markers; 1, native enzyme; 2, wild-type enzyme; 3, mutant with M57L; 4, mutant with M57T; 5, mutant with M57A.

```

      P8
1  ATGTCCTACCAACCACCTTA TGGAGT CGACG CCGCTCAGGTT CCTCAGGAAGAATTTGAC 60
1  M  S  Y  Q  P  L  I  G  V  D  A  A  Q  V  P  Q  E  E  F  D  20

      P1
61  CAGGAATTGAAAAACAAGCATT T CAGTACACTTATGATAATGGC GGAAATACGAGTTC 120
21  Q  E  L  K  N  K  H  E  Q  Y  T  Y  D  N  G  W  K  Y  E  F  40

121  CATGTTCCCAATGACAAACGAAT GTATACTCGA TCATGGGGGGCCAA GGCTGGACGG 180
41  H  V  P  N  D  K  R  I  V  Y  S  I  H  G  G  P  M  A  G  R  60

      P6
181  CACAACCTT CAGACATGTTACTACGACAGAGT CAGCAAAAATTTA CCGAACTCAATTCC 240
61  H  N  F  Q  T  C  Y  Y  Q  R  V  R  K  N  L  W  Q  V  N  W  80

      P5
      P7
      P4
241  TTAGAAGAAACTGGAACCG TGTGTCGTTGATTT GGATATTGAAAATAAACGTATTACT 300
81  L  E  T  G  T  V  V  S  L  I  L  D  I  E  N  K  R  I  T  100

301  ACGIICATGGCGI I I I CIGAGGG CATTGGGAGCATCCAGAGCAAGCAGACGGAGACAAG 360
101  T  F  M  A  F  S  Q  G  H  W  E  H  P  E  Q  A  H  G  D  K  120

361  CGGGAAGA TTGGACGGTGGAGAGAGCTTTCTAGAATTGAATTGCAACCAATAGGTAC 420
121  R  E  D  L  E  R  W  R  E  L  S  R  I  G  I  A  T  N  R  Y  140

421  TTGATAACCGAACAAGCATCGATCGATGAGATTT TGAAGCAAGAGGTGATTTACCTGAT 480
141  L  I  T  E  Q  A  S  I  D  E  I  F  E  G  R  G  D  L  P  D  160

481  ATTTCAATGGATCTACCAACGTTATAAGTATATA GTGAATTGAAGCCAATCAGGTTG 538
161  I  S  L  D  L  P  T  L  *  168

```

Fig. 3-2 Nucleotide and deduced amino acid sequences of CgPAD. The primers used for cloning the CgPAD gene are indicated by arrows above the nucleotide sequence. Dotted underlines indicate deduced amino acid sequences identical to those of the peptides derived from CNBr and *S. aureus* V8 protease digestions of native CgPAD. The residues possibly involved in the catalysis, which are integrally conserved in LpPAD (Rodríguez et al. 2010), are boxed.

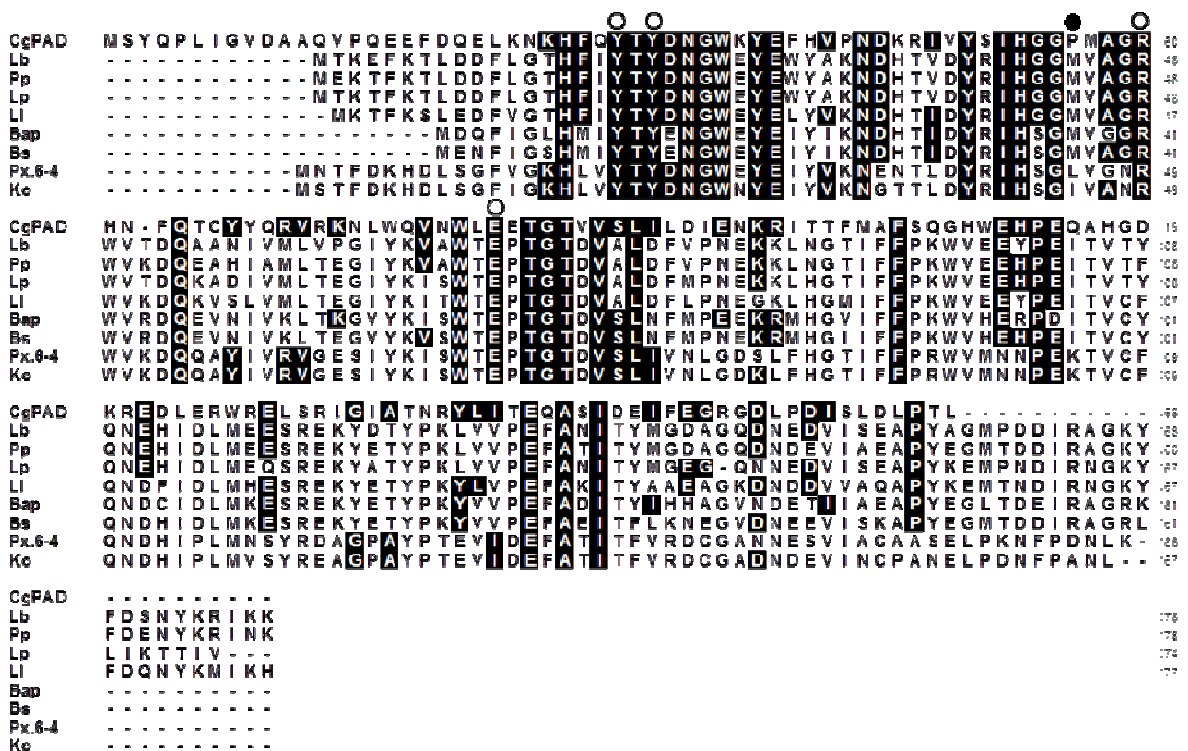


Fig. 3-3 Multiple amino acid sequence alignment of CgPAD with functional PADs reported to date. The sequences used are *L. brevis* ATCC 367 (RM84) (Lb; ABJ63379), *P. pentosaceus* ATCC 25745 (Pp; AJ276891), *L. plantarum* WCFS1 (Lp; PDB code 2GC9; gi93279967), *L. plantarum* LPCHL2 (Li; U63827), *B. pumilus* ATCC 15884 (*Bap*; AJ278683), *B. subtilis* 168 (Bs; AF017117), *Enterobacter* sp. Px6-4 (Px6-4; ACJ26748), and *K. oxytoca* (Ko; BAF65031). The sequences were aligned using the ClustalW program. Residues identical to those in CgPAD are shaded. Possible catalytic residues are indicated as open circles above the CgPAD sequence. Partially conserved Met residues are indicated as filled circle. Sequences of homologous hypothetical proteins of unknown function in the reported genome sequences are not included in the multiple alignments.

subtilis 168 (Cavin et al. 1998) with 26%, *Lactobacillus brevis* ATCC 367 (RM84) (Landete et al. 2010) with 25%, *P. pentosaceus* ATCC 25745 (Barthelmebs et al. 2001) with 25%, and *B. pumilus* ATCC 15884 (Barthelmebs et al. 2001) with 24% identity. Nevertheless, four residues (Tyr18, Tyr20, Arg48, and Glu71) involved in the catalysis of LpPAD (Rodríguez et al. 2010) were well conserved in CgPAD as Tyr30, Tyr32, Arg60 [Asn23 in the crystal structure of *Enterobacter* enzyme (Gu et al. 2011b)], and Glu82 and of PADs from other bacteria as these residues at the corresponding positions.

Construction of model structure and mutant proteins of CgPAD

The absence and/or replacement of methionine residues adjacent to catalytic residues or in the proximate area of active-site pockets has been reported to confer resistance to oxidation, as based on the catalytic activity of enzymes (Estell et al. 1985; Hagihara et al. 2001, 2003; Nonaka et al. 2003). Further, we demonstrated that the replacement or oxidation of such the Met residues altered the conversion rates of substrates by some enzymes (Hagihara et al. 2001, 2003; Nonaka et al. 2003, 2004; Saeki et al. 2007). Then, we first postulated that the fluctuation of the ratio of decarboxylation toward FA to PCA might result from oxidation of heat-labile CgPAD, because the deduced amino acid sequence contained two oxidizable Met residues at positions 57 and 103 (Fig. 3-2). It was expected that the replacement of either Met57 or Met 103 with the non-oxidizable amino acids would increase the ratio of decarboxylation activity of CgPAD toward FA to PCA.

According to this scenario, we constructed a model of CgPAD using the crystal structure of LpPAD (PDB code 2GC9) as the template. In the result, the Met residues at positions 57 and 103 in the modeled CgPAD appeared to be located in the active-site pocket and in the vicinity

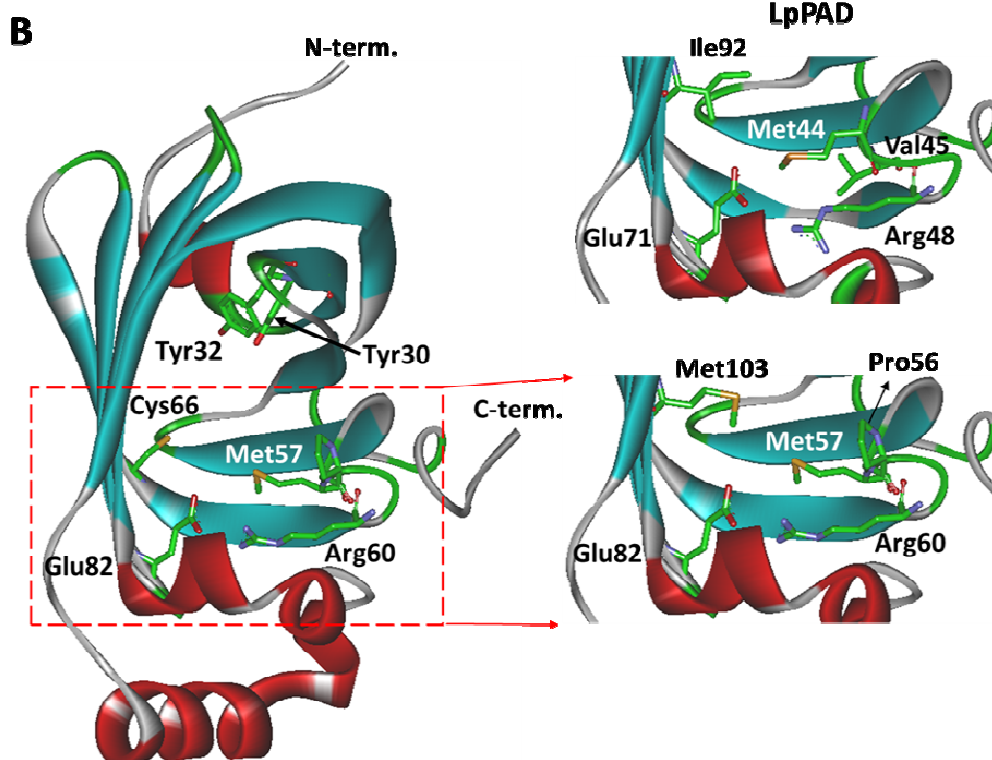
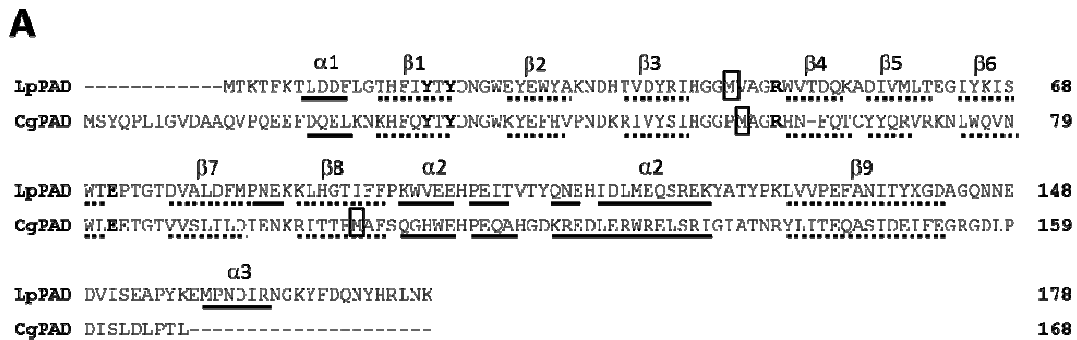


Fig. 3-4 A. Structure-based amino acid sequence alignment of CgPAD with LpPAD of known structure (PDB code 2GC9). The secondary structure prediction of the CgPAD sequence was done by the method of Kabsch and Sander (1983). The helices of LpPAD and CgPAD are shown by lines and b-strands in dotted lines. The methionine residues possibly close to active sites are boxed. **B.** A model structure of CgPAD incorporating possible catalytic residues Glu82 and Arg60 residues and subsite residues Tyr30 and Tyr32, along with Met57 and Cys66. It was constructed with the LpPAD structure as a template. The right plates indicate part of the active-site pocket around Met57 (Val45), Met103 (Ile92), and Pro56 (Met44) in the vicinity of possible catalytic residues Glu82 (Glu71) and Arg60 (Arg48) (numbers in parentheses correspond to residues in LpPAD).

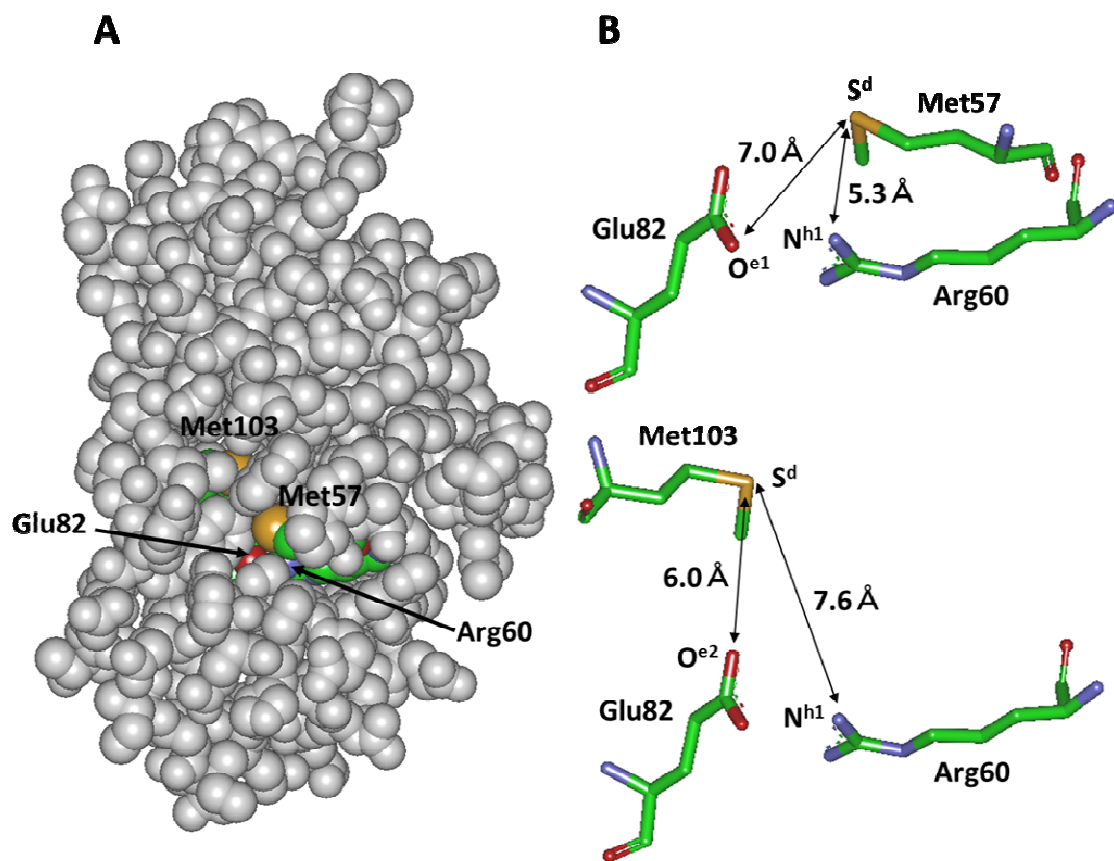


Fig. 3-5 **A.** A CPK model of CgPAD. The possible catalytic residues Arg60 and Glu82, along with Met57 and Met103, are shown. They are indicated by arrows. Cys66 is located at the other side of the model structure shown. **B.** Coordination of the catalytic residues in the surrounding Met57 (upper) and Met103 (lower) in the model CgPAD structure. The figures are stick models showing the distance from the respective catalytic residues to the S^d atom of either Met57 (upper) or Met103 (lower).

of possible catalytic residues Arg60 and Glu82 (Fig. 3-4). However, the Met103 residue is spatially more distant from the two catalytic residues and located deeper in the active-site pocket (Fig. 3-5). In contrast, the Met57 is located at the entrance of the pocket and in the immediate vicinity of the two catalytic residues. One of substrate-binding residues, Leu45, in the *Enterobacter* enzyme (Gu et al. 2011b) is conserved as Met at the corresponding positions in other aligned bacterial enzymes. The corresponding residue is replaced with Pro at position 56 and the adjacent residue is Met57 in CgPAD (Fig. 3-3).

Therefore, we selected the Met57 residue as the target for site-directed mutagenesis. Expecting that replacement of Met57 with a non-oxidizable amino acid would drastically increase the ratio of decarboxylation activity of CgPAD toward FA to PCA, we created mutant enzymes with M57L, M57T, and M57A and expressed them in *E. coli* cells. The recombinant wild-type and mutant enzymes, together with the native enzyme from *C. guilliermondii*, were each purified to homogeneity (Fig. 3-1). However, as shown in Table 3-2, the increase in the ratio of decarboxylation toward FA to PCA of the M57L mutant enzyme was not observed compared with those of the native and wild-type enzymes. The activities toward both substrates of the mutants with M57T and M57A were practically negligible.

Acceleration of FA decarboxylation activity of CgPAD by thiol compounds

For measurement of enzyme activities in the cell-free extracts, we disrupted the cells in the extraction buffer supplemented with 1 mM DTT. Then, we examined the effect of this thiol on the activity of purified native CgPAD. Unexpectedly, the FA decarboxylation activity was found to be enhanced by DTT at 0.2–1 mM (Fig. 3-6). The PCA decarboxylation activity was not affected by DTT at the concentrations examined.

To explain the unexpected positive effect of DTT, we next examined the effects of various

Table 3-2 Substrate specificities of native and recombinant enzymes

Enzyme	Substrate	Specific activity (U mg ⁻¹)	Relative activity ^a (%)
Native	FA	378 ± 16	100
	PCA	393 ± 6	104
	CA	53 ± 9	14
Recombinant	Wild-type		
	FA	260 ± 30	100
	PCA	259 ± 4.0	100
	CA	31.7 ± 2.8	12
	M57L		
	FA	20.1 ± 0.3	100
	PCA	20.5 ± 0.3	102
	CA	2.93 ± 0.03	15
	M57T		
	FA	< 0.1	—
	PCA	< 0.1	—
	CA	< 0.01	—
	M57A		
	FA	< 1.0	—
	PCA	< 1.0	—
CA	< 0.02	—	

^a The FA decarboxylation activities of the native and recombinant enzymes are taken as 100% for each.

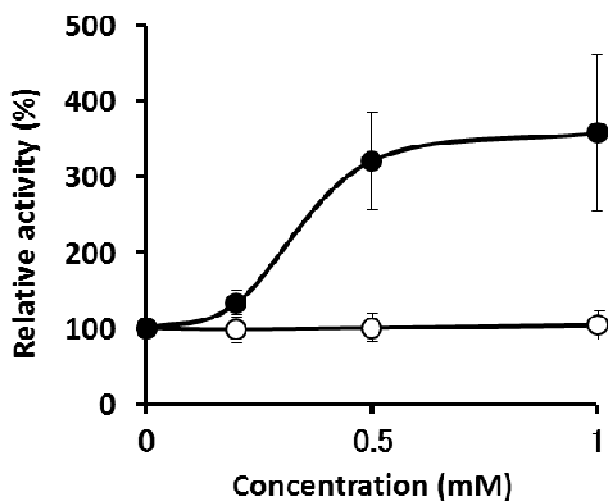


Fig. 3-6 Effect of DTT on decarboxylation activities toward FA and PCA of purified native CgPAD. DTT (0.2, 0.5, or 1 mM) was added to the reaction mixtures containing $\times 10$ enzyme (1.0-ml final volume) and incubated at 25°C for 20 min. An aliquot (0.1 ml) was withdrawn and added to 0.9 ml of the reaction mixture containing 0.1 M FA or PCA, and the initial velocities of decarboxylation of FA (filled circle) and PCA (open circle) were measured under the standard conditions of enzyme assay. The values obtained from three separate experiments are shown and expressed as percentages, taking the activity of each untreated enzyme as 100%. The bars indicate the standard deviation at each point.

sulfur-containing amino acids and chemical reagents on both activities. Positive effects on the FA decarboxylation activity were also observed with 2-mercaptoethanol (5 mM) and sulfhydryl amino acids such as L-cysteine, D-cysteine, and DL-homocysteine (1 mM each), and the increases in the relative decarboxylation activities of FA to PCA reached 2:1 to 3:1 when compared with the control (without thiol), as shown in Table 3-3. Cystic acid (1 mM) was essentially without effect.

The possibility that the replacement of Met57 with Leu disrupted the structural rigidity of CgPAD has not yet been excluded because its specific activity was considerably lower than those of the native and wild-type enzymes (Table 3-2). However, the positive effect by L-cysteine (1 mM) on FA decarboxylation activity was also observed with the M57L mutant enzyme as well as with native and recombinant wild-type forms, as shown in Table 3-4. Essentially, L-cysteine was without effect on the decarboxylation activity toward CA of the wild-type enzyme. The activity toward CA of the M57L mutant enzyme was too low to evaluate the effect of L-cysteine.

Activation of FA decarboxylation activity by ultrafiltrate of cell-free extract

Finally, we supposed that *C. guilliermondii* inherently possessed a physiological thiol activator, which might have been removed during the enzyme purification. Then, we prepared an ultrafiltrate of the cell-free extract (Mr 10,000-cut-off) of induced *C. guilliermondii* cells and incubated it with native and recombinant CgPADs at 25°C for 20 min before enzyme assays. As the results shown in Fig. 3-7, the ultrafiltrate was found to remarkably increase the FA decarboxylation activities of both enzymes (approximately up to 5-folds) with an increase in its volume, while it exhibited little effect on their PCA and CA decarboxylation activities. The ultrafiltrate of the cell-free extract of recombinant *E. coli* did not exhibit such an activation

Table 3-3 Effects of thiol reagents on the activities of native CgPAD

Additive (1 mM)	Specific activity (U mg ⁻¹)		FA/PCA
	FA (%)	PCA (%)	
None	378±16 (100)	393±6 (100)	0.96
2-Mercaptoethanol (5 mM)	806±56 (213)	440±3 (112)	1.83
Dithiothreitol	1140±177 (302)	598±7 (112)	1.91
L-Cysteine	1130±37 (299)	437±39 (111)	2.59
D-Cysteine	1590±252 (421)	590±4 (150)	2.69
DL-Homocysteine	1830±354 (484)	628±9 (160)	2.91
Cysteic acid	557±30 (147)	593±9 (151)	0.94

Experimental conditions were the same as those described in Fig. 3-6

Table 3-4 Effects of L-cysteine on the activities of recombinant wild-type and M57L mutant CgPAD

Substrate	Specific activity (U mg ⁻¹)	Relative activity ^b (%)
Wild type		
FA	260 ± 9.0	100
FA + L-cysteine ^a	759 ± 156	292
PCA	259 ± 4.0	100
PCA + L-cysteine	257 ± 3.3	99
CA	31.7 ± 2.8	12
CA + L-cysteine	35.9 ± 3.5	14
M57L		
FA	20.1 ± 0.3	100
FA + L-cysteine ^a	66.7 ± 8.5	332
PCA	20.5 ± 0.3	100
PCA + L-cysteine	26.0 ± 2.7	127
CA	< 2.6	< 13
CA + L-cysteine	ND ^c	

Experimental conditions were the same as those described in Fig. 3-6. ^a Treated with 1 mM. ^b The activity toward FA is taken as 100%. ^c Not determined.

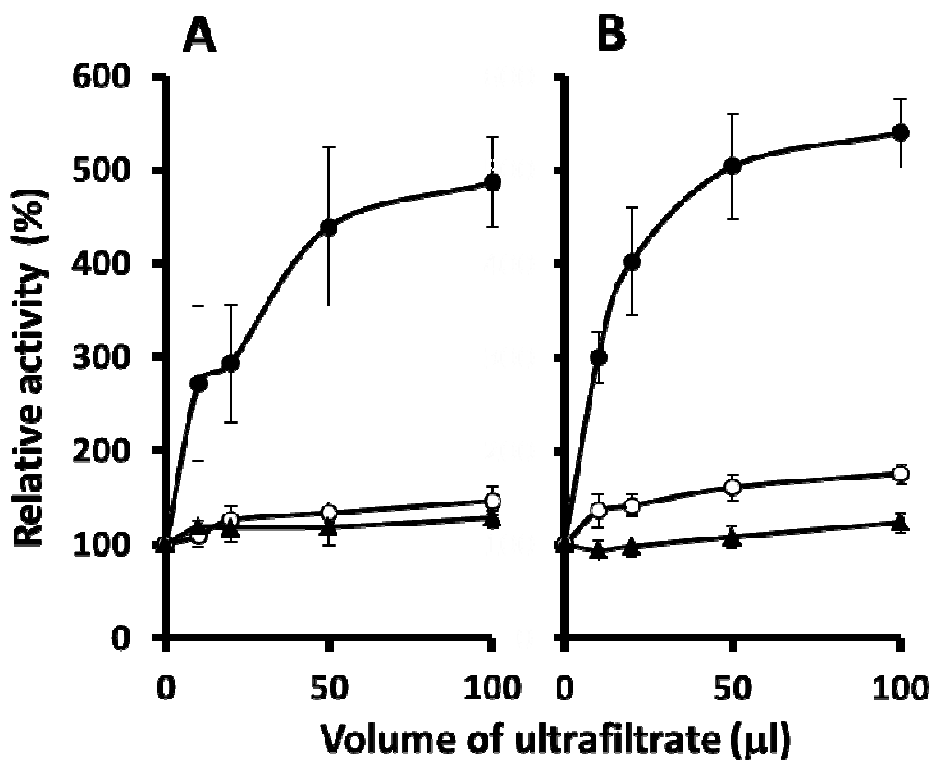


Fig. 3-7 Effect of ultrafiltrate on activities of native (A) and recombinant wild-type CgPAD (B). Cell pastes of 6H2N-induced *C. guilliermondii* and recombinant *E. coli* were disrupted with glass beads in the extraction buffer. The fresh cell-free extracts obtained (5.8–7.5 mg protein ml⁻¹) were ultrafiltered by centrifugation in an Amicon Ultra-15. Aliquots (10 μl to 100 μl) of the ultrafiltrate were added immediately to the reaction mixture containing enzyme (0.95-ml final volume), incubated at 25°C for 20 min, and then the initial velocities toward substrates were measured by adding 50 μl of a 0.1 M substrate. The values were obtained from several separate experiments and are expressed as percentages, taking the activity toward FA (filled circle), PCA (open circle), and CA (filled triangle) of the untreated enzyme as 100%.

effect. These results suggested that an unidentified activator was present in the *C. guilliermondii* cells.

Partial purification of true activator in the ultrafiltrate

The ultrafiltrate was subjected to gel-filtration chromatography on Bio-Gel P-2. As shown in Fig. 3-8, a possible true activator associated with the FA decarboxylation activity was detected in fractions corresponding to a M_r larger than 1,400. The fractions reacted positively with the 5,5'-dithio-bis(2-nitrobenzoic acid) (DTNB) and ninhydrin reagents. In the presence of 50 μ l of ultrafiltrate, the values of K_m , k_{cat} , and k_{cat}/K_m for FA were 5.67 mM, 278 s^{-1} , and 49.0 $s^{-1} mM^{-1}$, whereas those of the control (without ultrafiltrate) were 5.31 mM, 89.7 s^{-1} , and 16.9 $s^{-1} mM^{-1}$, respectively.

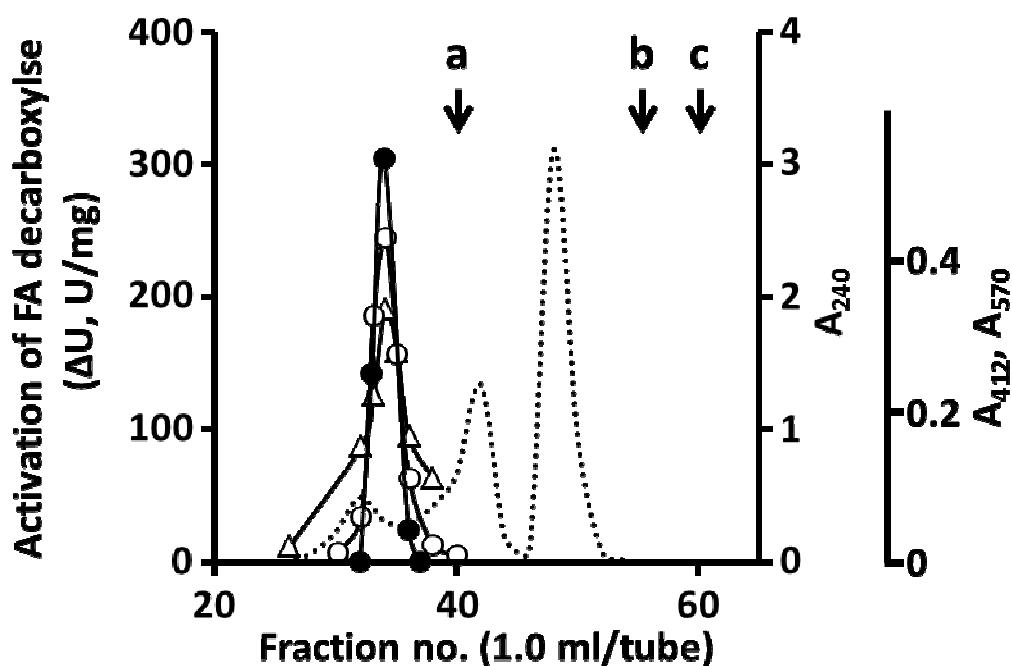


Fig. 3-8 Gel-filtration chromatography of ultrafiltrate. One ml of the ultrafiltrate prepared from the cell-free extract of induced *C. guilliermondii* cells was applied to a Bio-Gel P-2 column (1.0 cm × 50 cm) previously washed with distilled water and eluted with distilled water. The column was calibrated with cyanocobalamin (a, Mr = 1,355), cellobiose (b, Mr = 342), and glucose (c, Mr = 180), as indicated by vertical arrows. The elution pattern was monitored by measuring at 240 nm (dotted line). The fractions containing the activator of FA decarboxylase activity (filled circle) were examined for color reactions with DTNB solution at 412 nm (open circle) and ninhydrin solution at 570 nm (open triangle). The activation was expressed as $\Delta U \text{ mg}^{-1}$ [(activity + eluate) – (control activity)] after 20-min incubation at 25°C. For the color reactions, 0.1-ml aliquots were added to 0.9 ml of 5 mM DTNB in 50 mM phosphate buffer (pH 7.5) and ninhydrin solution, respectively.

Chapter 4 Discussion

In this study, we showed that a substrate-inducible CgPAD can be purified to homogeneity by a simple purification procedure within 3 days and that the purified enzyme was fully characterized. Our purification procedure does not include concentration of enzyme solution to subject to column chromatography on cation and anion exchangers equilibrated at an appropriate pH.

As shown in Chapter 2, the molecular mass of the purified CgPAD determined by SDS-PAGE is about 20 kDa, which is similar to those of yeast strains of *Brettanomyces anomalus* (Edlin et al. 1998) and *B. bruxellensis* (Godoy et al. 2008). The native CgPAD was a homodimer with two identical subunits, which is similar to those of the two yeasts (Edlin et al. 1998; Godoy et al. 2008) and bacteria such as *Bacillus subtilis* (Cavin et al. 1998), *B. pumilus* (Degrassi et al. 1995), and *Pseudomonas fluorescens* (Huang et al. 1994). Exceptionally, the PCA decarboxylase from *L. plantarum* LpCHL2 has a larger molecular mass of 93 kDa consisting of four identical 23.5-kDa subunits (Cavin et al. 1997b).

The purified CgPAD was active toward 4-hydroxycinnamic acid derivatives, PCA, FA, and CA, whose relative activity ratios are different from the PADs of *B. anomalus* and *B. bruxellensis* (Edlin et al. 1998; Godoy et al. 2008). Namely, it decarboxylated PCA, FA, and CA at relative ratios of 100:89:8, the values of which are very different from the enzymes of yeasts, *B. anomalus* (100:266:84) (Edlin et al. 1998) and *B. bruxellensis* (100:120:80) (Godoy et al. 2008). Further, the activity of CgPAD toward FA and/or PCA was stimulated by Mg^{2+} ions and their specific activities were much higher than those reported for these and other yeasts (Clausen et al. 1994; Edlin et al. 1998; Godoy et al. 2008; Mukai et al. 2010) and bacteria (Degrassi et al. 1995; Landete et al. 2010). The enzyme was inactive toward cinnamic acid, 2-

and 3-hydroxy-cinnamic acids, *o*- and *m*-cinnamic acids, and notably 3-(4-hydroxyphenyl)-propionic acid, indicating that the *p*-hydroxycinnamic acid (4-hydroxy-cinnamic acid) derivatives serve as substrates for this enzyme.

Characteristically, CgPAD was cold-adapted in that, even at 0°C, it exhibited more than 50% of the activity at the optimal temperature, which is similar to the *B. pumilus* enzyme (Degrassi et al. 1995). It was also heat-labile as in the cases of PADs from *B. pumilus* (Degrassi et al. 1995), *L. brevis* (Landete et al. 2010), and *L. plantarum* (Rodríguez et al. 2008).

The enzyme activity was abolished by *N*-bromosuccinimide and diethyl pyrocarbonate, suggesting that tryptophan and histidine residues contribute to the enzyme catalysis. It is generally accepted that tryptophan around an active site plays a role in substrate binding (Clarke 1987; Kawaminami et al. 1994) and histidine is essential for activity in some enzymes (Ito 2009). Heavy metal ions and 4-chloromercuribenzoate also inhibited the CgPAD activity completely. The contribution of cysteine residues to the catalysis is unclear because iodoacetate and *N*-ethylmaleimide exhibited either no or a moderately inhibitory effect, respectively.

PADs are believed to be responsible for the detoxification of phenolic acids, and most of them are inducible in yeasts (Clausen et al. 1994; Godoy et al. 2008; Goodey et al. 1982) and bacteria (Barthelmebs et al. 2000a, 2000b; Cavin et al. 1997b, 1998; Degrassi et al. 1995; Gury et al. 2009; Tran et al. 2008). The genetic mechanism of PAD expression has been well explained by the PadR-mediated response to phenol acids in bacteria such as *Pediococcus pentosaceus* (Barthelmebs et al. 2000b), *L. plantarum* (Gury et al. 2009), and *B. subtilis* (Tran et al. 2008). However, such the bacterial induction mechanism might not be applicable to eukaryotic *C. guilliermondii* ATCC 9058 because antimicrobial PCA and FA rather stimulated the growth rate of this yeast in YNB broth. The stimulation was reproducibly observed in the presence of both phenolic acids at concentrations from 0.1 mM to 2.0 mM, although they

significantly retarded growth at 10 mM.

The hyperinduction by 6H2N of PAD was first demonstrated by Hashidoko et al. (2001) using Gram-negative *Klebsiella oxytoca*. It seems likely that 6H2N can induce PADs in other eukaryotes and also those in Gram-positive bacteria if 6H2N were not degraded by the organisms. In fact, 6H2N was not degraded by *C. guilliermondii* ATCC 9058 in YNB broth as judged by HPLC (data not shown).

When *C. guilliermondii* ATCC 9058 was grown aerobically in YNB broth, stoichiometric conversions of FA and PCA to 4-VG and 4-VP, respectively, were completed within 24 h. 4-Ethylguaiaicol, 4-ethylphenol, and other derivatives from the products (Cavin et al. 1997a; Dias et al. 2003; Godoy et al. 2008; Suezawa and Suzuki 2007) were not detectable even after 2 days. Therefore, the reaction with CgPAD or fermentation using this yeast would allow industrial production of 4-VG and 4-VP, which are precursors to flavors and fragrances (Mathew and Abraham 2006; Priefert et al. 2001) and detected as the aroma of beers and wines (Coghe et al. 2004; Oelofse et al. 2008; Sáez et al. 2010; Smit et al. 2003; Thurston and Tubb 1981; Vanbeneden et al. 2008) and flavors of soy sauce and miso (Suezawa and Suzuki 2007).

In Chapter 3, we described for the first time the cloning, sequencing, and expressing the gene for a eukaryotic PAD in *E. coli*. CgPAD exhibited very low sequence similarity to reported functional PADs with 24–39% identity. CgPAD showed 100% amino acid sequence identity to a hypothetical protein (EDK35930; locus tag PGUG_00028) in the genome of the yeast *M. guilliermondii* ATCC 6260 (AAF000000000), and moderate similarity (51–56% identity) to the internal sequences of hypothetical proteins of unknown function in the genomes of fungi including the genera *Verticillium*, *Neosartorya*, *Aspergillus*, *Schizophyllum*, *Ustilago*, *Sporisorium*, *Nectria*, *Gibberella*, and *Penicillium*. Notably, CgPAD exhibited sequence

similarity to PAD1 (YDR538W) with less than 14% identity and essentially no homology with FDC1 (YDR539W) isolated from *S. cerevisiae* (Clausen et al. 1994; Mukai et al. 2010).

There was a possibility that either Met57 or Met103 in CgPAD was located in the active-site pocket and oxidized to methionine sulfoxide during growth or purification. Accordingly, the massive sulfoxide group of the oxidized Met residue in the CgPAD might hinder the entry of FA (4-hydroxy-3-methoxycinnamic acid) due to its 3-methoxy group, but not PCA (4-hydroxycinnamic acid), to the active-site pocket. To understand the fluctuation of the ratio of decarboxylation toward FA to PCA of CgPAD, we constructed a model structure of the enzyme and replaced the Met57 residue located at the entrance of the pocket with non-oxidizable amino acids by site-directed mutagenesis. However, a mutant enzyme (M57L) did not increase the decarboxylation ratio of FA to PCA, for instance. This may exclude the possibility that oxidation of Met57, close to the catalytic residues Arg60 and Glu82, alters the decarboxylation ratio of FA to PCA. A single Cys residue at position 66 could be responsible for the alteration of CgPAD activity. However, in the model of CgPAD we built, the Cys66 residue is located deeper in the active-site pocket and faced on the other side and far distant (7.2 Å) from the indole ring of Trp80 which might interact with Glu82. Essentially, conversion of cysteine to cysteic acid during purification steps is unlikely because cysteine is oxidized by strong chemical oxidants.

The activities toward substrates of the M57T and M57A mutants, together with M57L mutant, were found to be much lower than those of the native and recombinant wild-type forms of CgPAD. This result suggests that Met57 is one of the substrate-binding residues in the catalysis of CgPAD. In support of our view, one of substrate-binding residues, Leu45, in the *Enterobacter* PAD (Gu et al. 2011b) is conserved as Met at the corresponding positions in the aligned bacterial enzymes. The corresponding residue in CgPAD is Met57 in the model

structure of CgPAD (Fig. 3-4).

Unexpectedly, we found that the rate of FA decarboxylation activity, but not PCA decarboxylation activity, of CgPAD was accelerated by DTT, 2-mercaptoethanol, cysteine (both L- and D-forms), and DL-homocysteine, which are antioxidants and/or reducing reagents. However, these chemical reagents cannot reduce oxidized Met residues (methionine sulfoxide and methionine sulfonate) in protein molecules. Furthermore, L-cysteine and L-homocysteine are involved in the trans-sulfurization of amino acid metabolism (e.g., Brosnan and Brosnan 2006), both of which intracellular concentrations are very lowered by strict regulatory control. These results exclude the possibility that these amino acids are the physiological activator for CgPAD.

Finally, we found that an amino thiol-like endogenous factor in the ultrafiltrate of the *C. guilliermondii* cell-free extract drastically enhanced the FA decarboxylation activity. The kinetic data indicate that the ultrafiltrate increases the maximal activity toward FA without altering of the affinity to the substrate. These findings led us to conclude that a true activator for FA decarboxylation activity is inherently present in the *C. guilliermondii* cells. This also shows that the true activator was removed during the enzyme purification. Such a catalytic nature has never been reported in the literature. Identification of the structure of the endogenous activator would explain the novel catalytic feature of CgPAD and contribute to the clarification of physiological role of PADs in some yeast cells. It is interesting to examine whether such activation of eukaryotic PADs is observed by ultrafiltrates of prokaryotes and vice versa.

Rodríguez et al. (2010) clarified by site-directed mutagenesis of Arg48 and Glu71 in LpPAD that the entrance region, particularly the β 1– β 2 and β 3– β 4 loops, adopted a distinct closed conformation that decreased the opening of the active-site cavity. Possible subsite residues Tyr30 and Tyr32 and catalytic residue Glu82 along with Met57 of CgPAD are located

on the $\beta 1$ - $\beta 2$ loop and $\beta 3$ - $\beta 4$ loop, respectively (see Fig. 3-4 A). It is possible that the physiological activator in the ultrafiltrate and/or the tested thiol compounds induce conformational change of the loops so that the entry of FA is much easier than those of PCA and CA. CgPAD exhibits low sequence similarity to LpPAD of known structure, and we are crystalizing CgPAD to solve its X-ray structure.

Summary

A heat-labile phenolic acid decarboxylase (PAD) from *Candida guilliermondii* (*Meyerozyma guilliermondii*) was purified to homogeneity by simple successive column chromatographies within 3 days. The molecular mass was 20 kDa by SDS-polyacrylamide gel electrophoresis and 36 kDa by gel-filtration chromatography, suggesting that the purified enzyme was a homodimer. The optimal pH and temperature were approximately 6.0 and 25°C. Characteristically, more than 50% of the optimal activity was observed at 0°C, suggesting that this enzyme was cold-adapted. The enzyme converted *p*-coumaric acid (PCA), ferulic acid (FA), and caffeic acid to corresponding products with high specific activities of approximately 600, 530, and 46 U/mg, respectively. The activity was activated by Mg²⁺ ions, while it was completely inhibited by Fe²⁺, Ni²⁺, Cu²⁺, Hg²⁺, 4-chloromercuribenzoate, *N*-bromosuccinimide, and diethyl pyrocarbonate.

The enzyme was inducible and expressed inside the cells moderately by FA and PCA and significantly by non-metabolizable 6-hydroxy-2-naphthoic acid. Then the gene for this eukaryotic enzyme was cloned, sequenced, and expressed in *Escherichia coli* for the first time. The structural gene contained an open reading frame of 504 bp, corresponding to 168 amino acids with a calculated molecular mass of 19,828 Da. The deduced amino acid sequence exhibited low similarity to those of functional PADs previously reported from bacteria with 24–39% identity and to those of PAD1 and FDC1 proteins from *Saccharomyces cerevisiae* with less than 14% identity.

Surprisingly, the ultrafiltrate (Mr 10,000-cut-off) of the cell-free extract of *C. guilliermondii* remarkably activated the FA decarboxylation by the purified enzyme, whereas it was almost without effect on the PCA decarboxylation. Gel-filtration chromatography of the ultrafiltrate suggested that an endogenous amino thiol-like compound with a molecular weight greater than Mr 1,400 was responsible for the activation.

References

- Ardiansyah, Ohsaki Y, Shirakawa H, Koseki T, Komai M (2008) Novel effects of a single administration of ferulic acid on the regulation of blood pressure and the hepatic lipid metabolic profile in stroke-prone spontaneously hypertensive rats. *J Agric Food Chem* 56:2825–2830
- Baranowski JD, Davidson PM, Nagel CW, Branen AL (1980) Inhibition of *Saccharomyces cerevisiae* by naturally occurring hydroxycinnamates. *J Food Sci* 45:592–594
- Barata A, Seborro F, Belloch C, Malfeito-Ferreira M, Loureiro V (2008) Ascomycetous yeast species recovered from grapes damaged by honeydew and sour rot. *J Appl Microbiol* 104:1182–1191
- Barthelmebs L, Diviès C, Cavin JF (2000a) Knockout of the *p*-coumarate decarboxylase gene from *Lactobacillus plantarum* reveals the existence of two other inducible enzymatic activities involved in phenolic acid metabolism. *Appl Environ Microbiol* 66:3368–3375
- Barthelmebs L, Diviès C, Cavin JF (2001) Expression in *Escherichia coli* of native and chimeric phenolic acid decarboxylases with modified enzymatic activities and method for screening recombinant *E. coli* strains expressing these enzymes. *Appl Environ Microbiol* 67:1063–1069.
- Barthelmebs L, Lecomte B, Diviès C, Cavin JF (2000b) Inducible metabolism of phenolic acids in *Pediococcus pentosaceus* is encoded by an autoregulated operon which involves a new class of negative transcriptional regulator. *J Bacteriol* 182:6724–6731
- Brosnan JT, Brosnan ME (2006) The sulfur-containing amino acids: an overview. *J Nutr* 136:1636S-1640S
- Cavin JF, Barthelmebs L, Diviès C (1997a) Molecular characterization of an inducible *p*-coumaric acid decarboxylase from *Lactobacillus plantarum*: gene cloning, transcriptional analysis, overexpression in *Escherichia coli*, purification and characterization. *Appl Environ Microbiol* 63:1939–1944
- Cavin JF, Barthelmebs L, Guzzo J, Beeumen JV, Samyn B, Travers JF, Diviès C (1997b) Purification and characterization of an inducible *p*-coumaric acid decarboxylase from *Lactobacillus plantarum*.

FEMS Microbiol Lett 147:291–295

Cavin JF, Dartois V, Diviès C (1998) Gene cloning, transcriptional analysis, purification, and characterization of phenolic acid decarboxylase from *Bacillus subtilis*. Appl Environ Microbiol 64:1466–1471

Clarke AJ (1987) Essential tryptophan residues in the function of cellulase from *Schizophyllum commune*. Biochim Biophys Acta 912:424–431

Clausen M, Lamb CJ, Megnet R, Doerner PW (1994) *PADI* encodes phenylacrylic acid decarboxylase which confers resistance to cinnamic acid in *Saccharomyces cerevisiae*. Gene 142:107–112

Coghe S, Benoot K, Delvaux F, Vanderhaegen B, Delvaux FR (2004) Ferulic acid release and 4-vinylguaiacol formation during brewing and fermentation: indications for feruloyl esterase activity in *Saccharomyces cerevisiae*. J Agric Food Chem 52:602–608

Degrassi G, Polverino de Laureto P, Bruschi CV (1995) Purification and characterization of ferulate and *p*-coumarate decarboxylase from *Bacillus pumilus*. Appl Environ Microbiol 61:326–332

Dias L, Dias S, Sancho T, Stender H, Querol A, Malfeito-Ferreira M, Loureiro V (2003) Identification of yeasts isolated from wine-related environments and capable of producing 4-ethylphenol. Food Microbiol 20:567–574

Donaghy JA, Kelly PF, McKay A (1999) Conversion of ferulic acid to 4-vinyl guaiacol by yeasts isolated from unpasteurised apple juice. J Sci Food Agric 79:453–456

Edlin DAN, Narbad A, Gasson MJ, Dickinson JR, Lloyd D (1998) Purification and characterization of hydroxycinnamate decarboxylase from *Brettanomyces anomalus*. Enzyme Microb Technol 22:232–239

Estell DA, Graycar TP, Wells JA (1985) Engineering an enzyme by site-directed mutagenesis to be resistant to chemical oxidation. J Biol Chem 260:6518–6521

Fallico B, Lanza MC, Maccarone E, Asmundo CN, Rapisarda P (1996) Role of hydroxycinnamic acids

- and vinylphenols in the flavor alteration of blood orange juices. *J Agric Food Chem* 44:2654–2657
- Godoy L, Martínez C, Carrasco N, Ganga MA (2008) Purification and characterization of a *p*-coumarate decarboxylase and a vinylphenol reductase from *Brettanomyces bruxellensis*. *Int J Food Microbiol* 127:6–11
- Goodey AR, Tubb RS (1982) Genetic and biochemical analysis of the ability of *Saccharomyces cerevisiae* to decarboxylate cinnamic acids. *J Gen Microbiol* 128:2615–2620
- Gu W, Li X, Huang J, Duan Y, Meng Z, Zhang KQ, Yang J (2011a) Cloning, sequencing, and overexpression in *Escherichia coli* of the *Enterobacter* sp. Px6-4 gene for ferulic acid decarboxylase. *Appl Microbiol Biotechnol* 89:1797–1805
- Gu W, Yang J, Lou Z, Liang L, Sun Y, Huang J, Li X, Cao Y, Meng Z, Zhang KQ (2011b) Structural basis of enzymatic activity for the ferulic acid decarboxylase (FADase) from *Enterobacter* sp. Px6-4. *PLoS ONE* 6(1): e16262
- Gury J, Seraut H, Tran NP, Barthelmebs L, Weidmann S, Gervais P, Cavin JF (2009) Inactivation of PadR, the repressor of the phenolic acid stress response, by molecular interaction with Usp1, a universal stress protein from *Lactobacillus plantarum*, in *Escherichia coli*. *Appl Environ Microbiol* 75:5273–5283
- Hagihara H, Hatada Y, Ozawa T, Igarashi K, Araki H, Ozaki K, Kobayashi T, Kawai S, Ito S (2003) Oxidative stabilization of an alkaliphilic *Bacillus* α -amylase by replacing single specific methionine residue by site-directed mutagenesis. *J Appl Glycosci* 50:367–372
- Hagihara H, Hayashi Y, Endo K, Igarashi K, Ozawa T, Kawai S, Ozaki K, Ito S (2001) Deduced amino-acid sequence of a calcium-free α -amylase from a strain of *Bacillus*. Implications from molecular modeling of high oxidation stability and chelator resistance of the enzyme. *Eur J Biochem* 268:3974–3982
- Hashidoko Y, Tanaka T, Tahara S (2001) Induction of 4-hydroxycinnamate decarboxylase in *Klebsiella*

- oxytoca* cells exposed to substrates and non-substrate 4-hydroxycinnamate analogs. *Biosci Biotechnol Biochem* 65:2604–2612
- Huang Z, Dostal L, Rosazza JP (1994) Purification and characterization of a ferulic acid decarboxylase from *Pseudomonas fluorescens*. *J Bacteriol* 176:5912–5918
- Huang MT, Smart RC, Wong CQ, Conney AH (1988) Inhibitory effect of curcumin, chlorogenic acid, caffeic acid, and ferulic acid on tumor promotion in mouse skin by 12-*O*-tetradecanoylphorbol-13-acetate. *Cancer Res* 48:5941–5946
- Igarashi K, Hatada Y, Hagihara H, Saeki K, Takaiwa M, Uemura T, Ara K, Ozaki K, Kawai S, Kobayashi T, Ito S (1998) Enzymatic properties of a novel liquefying α -amylase from an alkaliphilic *Bacillus* isolate and entire nucleotide and amino acid sequences. *Appl Environ Microbiol* 64:3282–3289
- Ito S (2009) Features and applications of microbial sugar epimerases. *Appl Microbiol Biotechnol* 84:1053–1060
- Jung EH, Kim SR, Hwang IK, Ha TY (2007) Hypoglycemic effects of a phenolic acid fraction of rice bran and ferulic acid in C57BL/KsJ-*db/db* mice. *J Agric Food Chem* 55:9800–9804
- Kabsch W, Sander C (1983) Dictionary of protein secondary structure: pattern recognition of hydrogen-bonded and geometrical features. *Biopolymers* 22:2577–2637
- Kawaminami S, Ozaki K, Sumitomo N, Hayashi Y, Ito S, Shimada I, Arata Y (1994) A stable isotope-aided NMR study of the active site of an endoglucanase from a strain of *Bacillus*. *J Biol Chem* 269:28752–28756
- Kurtzman CP, Suzuki M (2010) Phylogenetic analysis of ascomycete yeasts that form coenzymeQ-9 and the proposal of the new genera *Babjeviella*, *Meyerozyma*, *Millerozyma*, *Priceomyces*, and *Scheffersomyces*. *Mycoscience* 51:2–14
- Landete JM, Rodríguez H, Curiel JA, de las Rivas B, Mancheño JM, Muñoz R (2010) Gene cloning, expression, and characterization of phenolic acid decarboxylase from *Lactobacillus brevis* RM84. *J*

Ind Microbiol Biotechnol 37:617–624

- Lin FH, Lin JY, Gupta RD, Tournas JA, Burch JA, Selim MA, Monteiro-Riviere NA, Grichnik JM, Zielinski J, Pinnell SR (2005) Ferulic acid stabilizes a solution of vitamins C and E and doubles its photoprotection of skin. *J Invest Dermatol* 125:826–832
- Liu RH (2004) Potential synergy of phytochemicals in cancer prevention: mechanism of action. *J Nutr* 134: 3479S–3485S
- Maoka T, Tanimoto F, Sano M, Tsurukawa K, Tsuno T, Tsujiwaki S, Ishimaru K, Takii K (2008) Effects of dietary supplementation of ferulic acid and gamma-oryzanol on integument color and suppression of oxidative stress in cultured red sea bream, *Pagrus major*. *J Oleo Sci* 57:133–137
- Martorell P, Barata A, Malfeito-Ferreira M, Fernández-Espinar MT, Loureiro V, Querol A (2006) Molecular typing of the yeast species *Dekkera bruxellensis* and *Pichia guilliermondii* recovered from wine related sources. *Int J Food Microbiol* 106:79–84
- Mathew S, Abraham TE (2004) Ferulic acid: an antioxidant found naturally in plant cell walls and feruloyl esterases involved in its release and their applications. *Crit Rev Biotechnol* 24:59–83
- Mathew S, Abraham TE (2006) Bioconversions of ferulic acid, a hydroxycinnamic acid. *Crit Rev Microbiol* 32:115–125
- Mukai N, Masaki K, Fujii T, Kawamukai M, Iefuji H (2010) *PADI* and *FDCI* are essential for the decarboxylation of phenylacrylic acids in *Saccharomyces cerevisiae*. *J Biosci Bioeng* 109:564–569
- Nonaka T, Fujihashi M, Kita A, Hagihara H, Ozaki K, Ito S, Miki K (2003) Crystal structure of calcium-free α -amylase from *Bacillus* sp. strain KSM-K38 (AmyK38) and its sodium binding sites. *J Biol Chem* 278:24818–24824
- Nonaka T, Fujihashi M, Kita A, Saeki K, Ito S, Horikoshi K, Miki K (2004) The crystal structure of an oxidatively stable subtilisin-like alkaline serine protease, KP-43, with a C-terminal β -barrel domain. *J Biol Chem* 279:47344–47351

- Oelofse A, Pretorius IS, du Toit M (2008) Significance of *Brettanomyces* and *Dekkera* during winemaking: a synoptic review. *S Afr J Enol Vitic* 29:128–144
- Pereira RS, Mussatto SI, Roberto IC (2011) Inhibitory action of toxic compounds present in lignocellulosic hydrolysates on xylose to xylitol bioconversion by *Candida guilliermondii*. *J Ind Microbiol Biotechnol* 38:71–78
- Priefert H, Rabenhorst J, Steinbüchel A (2001) Biotechnological production of vanillin. *Appl Microbiol Biotechnol* 56:296–314
- Rodríguez H, Angulo I, de Las Rivas B, Campillo N, Páez JA, Muñoz R, Mancheño JM (2010) *p*-Coumaric acid decarboxylase from *Lactobacillus plantarum*: structural insights into the active site and decarboxylation catalytic mechanism. *Proteins* 78:1662–1676
- Rodríguez H, Landete JM, Curiel JA, de las Rivas B, Mancheño JM, Muñoz R (2008) Characterization of the *p*-coumaric acid decarboxylase from *Lactobacillus plantarum* CECT 748^T. *J Agric Food Chem* 56:3068–3072
- Saeki K, Ozaki K, Kobayashi T, Ito S (2007) Detergent alkaline proteases: enzymatic properties, genes, and crystal structures. *J Biosci Bioeng* 103:501–508
- Sáez JS, Lopes CA, Kirs VC, Sangorrin MP (2010) Enhanced volatile phenols in wine fermented with *Saccharomyces cerevisiae* and spoiled with *Pichia guilliermondii* and *Dekkera bruxellensis*. *Lett Appl Microbiol* 51:170–176
- Sali A, Blundell TL (1993) Comparative protein modeling by satisfaction of spatial restraints. *J Mol Biol* 234:779–815
- Smit A, Cordero Otero RR, Lambrechts MG, Pretorius IS, van Rensburg P (2003) Enhancing volatile phenol concentrations in wine by expressing various phenolic acid decarboxylase genes in *Saccharomyces cerevisiae*. *J Agric Food Chem* 51:4909–4915
- Sri Balasubashini M, Rukkumani R, Menon VP (2003) Protective effects of ferulic acid on

- hyperlipidemic diabetic rats. *Acta Diabetol* 40:118–122
- Stead D (1995) The effect of hydroxycinnamic acids and potassium sorbate on the growth of 11 strains of spoilage yeasts, *J Appl Bacteriol* 78:82–87
- Steers Jr E, Craven GR, Anfinsen CB (1965) Evidence for nonidentical chains in the β -galactosidase of *Escherichia coli* K12. *J Biol Chem* 240:2478–2484
- Suezawa Y, Suzuki M (2007) Bioconversion of ferulic acid to 4-vinylguaiacol and 4-ethylguaiacol and of 4-vinylguaiacol to 4-ethylguaiacol by halotolerant yeasts belonging to the genus *Candida*. *Biosci Biotechnol Biochem* 71:1058–1062
- Sutherland JB, Tanner LA, Moore JD, Freeman JP, Deck J, Williams AJ (1995) Conversion of ferulic acid to 4-vinylguaiacol by yeasts isolated from frozen concentrated orange juice. *J Food Protect* 58:1260–1262
- Thompson JD, Gibson TJ, Plewniak F, Jeanmougin F, Higgins DG (1997) The Clustal_X windows interface: flexible strategies for multiple sequence alignment aided by quality analysis tools. *Nucl Acids Res* 25:4876–4882
- Thurston PA, Tubb RS (1981) Screening yeast strains for their ability to produce phenolic off-flavours: a simple method for determining phenols in wort and beer. *J Inst Brew* 87:177–179
- Tran NP, Gury J, Dartois V, Nguyen TKC, Seraut H, Barthelmebs L, Gervais P, Cavin JF (2008) Phenolic acid-mediated regulation of the *padC* gene, encoding the phenolic acid decarboxylase of *Bacillus subtilis*. *J Bacteriol* 190:3213–3224
- Uchiyama H, Hashidoko Y, Kuriyama Y, Tahara S (2008) Identification of the 4-hydroxycinnamate decarboxylase (PAD) gene of *Klebsiella oxytoca*. *Biosci Biotechnol Biochem* 72:116–123
- Van Beek S, Priest FG (2000) Decarboxylation of substituted cinnamic acids by lactic acid bacteria isolated during malt whisky fermentation. *Appl Environ Microbiol* 66:5322–5328
- Vanbeneden N, Gils F, Delvaux F, Delvaux FR (2008) Formation of 4-vinyl and 4-ethyl derivatives from

hydroxycinnamic acids: occurrence of volatile phenolic flavour compounds in beer and distribution of Pad1-activity among brewing yeasts. *Food Chem* 107:221–230

Zago A, Degrassi G, Bruschi CV (1995) Cloning, sequencing and expression in *Escherichia coli* of the *Bacillus pumilus* gene for ferulic acid decarboxylase. *Appl Environ Microbiol* 61:4484–4486

Acknowledgements

First of all, I am grateful to Prof. Susumu Ito, Department of Bioscience and Biotechnology, Faculty of Agriculture, University of the Ryukyus, for his teaching, encouragement, and valuable comments made on my research. I sincerely thank Dr. Toki Taira in this laboratory for the kind concern, encouragement and lots of help in my daily life. I also thank colleagues of our laboratory for helping this study.

I would like to thank Prof. Emeritus Masaaki Yasuda and Prof. Hirohide Toyama in this Department for their value comments. Especially, Prof. Toyama suggested to my work and read my manuscript critically.

Thanks are also to Prof. Toshihiko Suganuma, Department of Biochemical Sciences and Technology, Faculty of Agriculture, Kagoshima University, and Prof. Keiichi Watanabe, Department of Applied Biochemistry and Food Science, Faculty of Agriculture, Saga University, for their helpful advices and critical reading of my manuscript.

I would like to acknowledge the Heiwa Nakajima Foundation Scholarship for financial support in part.

Finally, I would like to thank my family for continuous support and encouragement during the course of my research in a lot of ways.